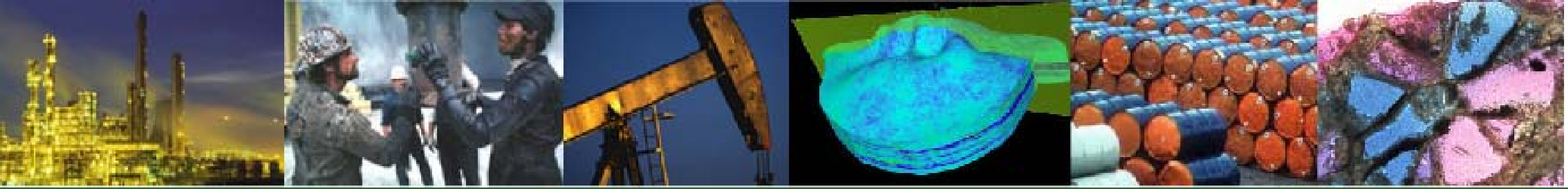

SIMULATION EVALUATION OF CO2 FLOODING IN THE MUDDY RESERVOIR, GRIEVE FIELD, WYOMING

Shaochang Wo and Peigui Yin

Enhanced Oil Recovery Institute
University of Wyoming

October 2007

Table of Contents **Page**

Introduction/Disclaimer

This report was prepared as an account of a collaborative study between the Enhanced Oil Recovery Institute (EORI) of the University of Wyoming and the Elk Petroleum, Inc. (Elk Petroleum). The objective of the study is to assess the EOR potential of CO2 flooding in Grieve Muddy reservoir, an oil reservoir in Natrona County of Wyoming, owned by Elk Petroleum. The results from the study were documented in three separate reports: "Stratigraphic Core Study of the Muddy Formation", prepared by Beverly Blakeney DeJarnett, "Diagenesis of Muddy Sandstones", prepared by Peigui Yin, and this report on simulation of history matching & CO2 flooding forecast. All opinions and simulation forecasts in this report are based on available data considered to be reliable. Neither EORI nor the authors makes any warranty or assumes any legal liability or responsibility of the accuracy of the predictions in this report.

Summary of Results

The simulation evaluation concluded that gravity stable CO2 flooding can be an effective EOR method for the Grieve Muddy reservoir. Up to 23 MMBO could ultimately be recovered by gravity stable CO2 flooding. The reservoir has potential to sequester more than 145 BSCF of CO2 at the end of CO2 flooding operation. Prior to the simulation of history matching and CO2 flooding, a four-layer Petrel model of Grieve Muddy reservoir was developed based on the identified facies in the Muddy channel sand and the overlain sandstone interval of bay-head delta deposition. Porosity and permeability distributions of layers generated in the Petrel model were exported to the simulation model. An OOIP estimation of 67 MMBO in Grieve Muddy channel sand has resulted from a simulation history matching based on the full-field material balance. History matching also reveals that about one MMSTBO of oil and 8.2 BSCF of gas have moved down from the overlain low-permeability sandstone interval into the Muddy channel sand interval during the reservoir depletion.

Three representative scenarios are used in this report to demonstrate the performance of gravity stable CO2 flooding under different CO2 injection schemes. To repressurize the reservoir to an operation pressure above the MMP, 90 BSCF or more of CO2 would need to be injected before any production. The initial CO2 demand is estimated to be in the 50,000 to 110,000 MSCF/day range. The repressurization phase could last 2.25 to 6 years, in the simulated cases, depending on CO2 injection volume rates. Total CO2 purchased are estimated to be in the 119 to 188 BSCF range depending on the operation duration and CO2 injection rate. It is estimated that between 20 and 23 MMBO could be produced by a 30-year operation of CO2 flooding while about 80% of the recoverable oil would be produced within the first 5 to 6 years of production. The net CO2 usage efficiency, the ratio between total purchased CO2 and total produced oil, varies from 7.3 to 8.1 MSCF/BO in the simulated cases.

3D Petrel Reservoir Model

Discovered in 1954, Grieve oil field is located in southeastern Wind River Basin, central Wyoming. This lower Cretaceous, valley-filled and channelized, Muddy sandstone reservoir is a stratigraphic/structural trap with an average structural dip of 15 degrees [3, 4]. The reservoir has a depth of about 6,900 ft, and is on top of a known down-dip aquifer. Three distinct lithofacies are identified within the Muddy channel sandstone at Grieve Field [1], which is overlain by a low-permeability mudstone/sandstone interval of bay-head delta deposition. The oil producing channel sand has an average porosity of 20.4% and average permeability of 220 md from core measurements [5]. The Muddy sand at Grieve Field appears to be weakly water-wet as reported from a wettability study [6]. In this study, prior to the simulation of history matching and CO2 flooding, a 3D model of Grieve Muddy reservoir was developed in the Petrel platform, a geologic modeling package from Schlumberger.

Description of Well Porosity, Permeability, and Facies Tops. Beverly Blakeney DeJarnett has identified three facies within the Muddy channel sand, named Facies A, Facies B and Facies C. They are typically overlain one upon another in the Grieve field area. An additional two mudstone and mudstone/sandstone lithofacies were also identified, named Facies D and E, in the interval of bay-head delta deposition above the Muddy channel sand [1]. Well tops of facies, picked by Chris Mullen of Elk Petroleum, were used for layering and calculating the average porosity and permeability of facies. Table 1 includes the facies tops and the calculated porosity and permeability averages in wells that have measured core porosity and permeability. As given in Figure 1, the average porosity in facies A, facies B, and facies C are 22.1%, 18.7%, and 13.5%, respectively. The average permeability in facies A, facies B, and facies C are 404 md, 338 md, and 14.1 md, respectively.

A Four-Layer Reservoir Model. Based on the well tops of facies, a 3D model of the Grieve Muddy reservoir was constructed in Petrel platform. The model consists of four layers (zones). Three lower layers are the facies A, B, and C intervals in the Muddy channel sand. The top layer consists of facies D and E, which are marine-affected mudstones, bioturbated siltstones and sandstones between the Muddy sandstone top and the top of facies C. Functional Interpolation, a mapping method, was used to generate the 3D surfaces of layer tops. Figure 2 shows a 3D view of original fluid distributions where the gas-oil contact is set at 675 ft above the sea level and oil-water contact is set at -73 ft below the sea level. The Muddy channel sand pinches out at the structure top as shown in Figure 3 from a bottom view of the grid pore volume distribution.

Isochore Maps. Exported from the Petrel model, Figure 4 shows the isochore map of Grieve Muddy channel sand, which is the contour map of true vertical thickness between the top of Facies C and the base of Facies A. The thickness of the channel sand varies from 10 ft to more than 110 ft in the northern part of the field. Figure 5 shows the isochore map of the top layer consisting of Facies D and E. In contrast, the overlain layer is thicker at the structure top where the channel sand pinches out.

Porosity and Permeability Distributions. Synthetic porosity and permeability logs were created to represent average porosity and permeability of facies intervals in wells and were used as mapping control points. For wells that don't have lab-measured porosity and permeability for some or all of facies intervals, the facies average porosity and permeability were assumed, Table 1 and Figure 1. Sequential Gaussian Simulation, a mapping method, was used to generate the porosity and permeability distributions within each layer. 3D views of porosity and permeability distributions for each layer are shown in Figure 6-9 and Figure 10-13, respectively.

Volumetric Estimates of Original Oil-in-Place. Petrel's Volume Calculation Utility was used to calculate the original oil-in-place (OOIP) for the Grieve Muddy reservoir. With different assumptions of gas-oil and oil-water contact depths and initial saturation distributions, the OOIP in the Muddy channel sand was estimated between 54 to 68 MMSTOB. Models with those assumptions were later tested to match the field production history. It appears from history matching, discussed in the following section, that an estimate of 67 million barrel OOIP in the Muddy channel sand is most credible. Observed from reservoir cores, oil also exists in the low-permeability sandstone interval overlain the Muddy channel sand. Because of the lack of sufficient log or core data, a volumetric estimate of OOIP for the top layer is difficult and, therefore, it is subject to production history matching to provide an estimation of effective OOIP.

Reservoir Grid System. The grid configuration resulting from a geologic model in Petrel can directly be exported to a grid description file in Eclipse format. In generating a grid system for the Grieve Muddy reservoir, the coordinate system was rotated 45 degree counterclockwise to reduce the number of inactive cells. The final exported grid system contains a total of 78,432 cells, in which 47,671 are active cells. A bottom view of the reservoir model, Figure 3, shows the grid pore volume distribution above the oil-water contact.

Original and Current Oil-in-Place Estimation

The OOIP in the Muddy channel sand was estimated between 54 to 68 MMSTOB from the 3D Petrel model, depending on assumptions of gas-oil and oil-water contact depths and initial saturation distributions. In the next step, a simulation of history matching is needed to verify those assumptions and to predict current oil-in-place. Using the grid configuration and distributions of porosity and permeability resulted from the Petrel model, Eclipse simulation models were created as candidate models for the Grieve Muddy reservoir. Since discovered in 1954, Grieve Field has produced about 30 million barrels of oil, 32.6 million barrels of water, and more than 109 BCF of gas. The oil is a premium light sweet crude of 37 degree API gravity. Figure 14 shows the monthly production history of Grieve Field. The recovery mechanisms include gas expansion, down-dip water drive, and pressure maintenance by re-injecting produced gas into the field's gas cap. Reservoir blow down started in 1977 when field water-oil production ratio increased to 90%. Consistent measurements from pressure build-up tests, Figure 15, indicate a good reservoir communication. Because the reservoir can be described by a typical "tank model", for the simulation model, getting a good match in reservoir pressure reflects an appropriate material balance in the simulated reservoir. While the black-oil simulator of Eclipse Parallel, installed on EORI's 15-node HP cluster, was used for history matching, the Eclipse compositional simulator was used to simulate CO_2 flooding.

Well Production Controls in History Match. In matching well production history, either the bottom-hole flow pressure or a fluid rate is commonly used as the well production control. As for Grieve Field, no record of well bottom-hole flow pressure is available and, prior to any water production, some of the gas production data are also missing. Therefore, oil production rate is the only reliable data that can be used for well production control, especially in the initial 5 to 6 years of production. However, when water became the dominant fluid produced from some of the wells in the late 1960s and during the blow-down, the simulation model under oil-rate control has difficulty producing enough water. To overcome this difficulty, a liquid rate or reservoir volume rate may have to be used as well production control and, most likely, permeability and relative permeability at local producing cells may need to be adjusted in order to match both oil and water rates . Because of the time restriction on this study, we used a different approach that doesn't require a match in water production. Instead of doing well-by-well history match, the focus was to match the history of average reservoir pressure and to achieve an overall material balance in the reservoir.

Simulation of Reservoir Material Balance. The Grieve Muddy reservoir is believed to be hydraulically connected, in which the expansion of remaining oil and gas depends only on the reservoir pressure. During the course of production, for any given time the material balance in reservoir can be described by

[change in reservoir pore volume] = [change in oil volume] + [change in free gas volume] + [change in water volume]

Where the change in water volume is determined by initial and current water in reservoir, the amount of produced water, and the water influx from aquifer.

[change in water volume] = [water influx from aquifer] + [initial water in reservoir] – [produced water] – [current water in reservoir]

Because no water was produced from Grieve Muddy reservoir in the first 5-6 years of production, the reservoir initially contained only connate water. Therefore, any subsequently produced water actually came from the aquifer as part of the influxed water. In the simulation of reservoir material balance, the change in water volume depends only on the net volume of influxed water that currently remains in the reservoir.

[change in water volume] = [the net volume of influxed water currently in reservoir]

A simulation starts with any one of the candidate models that has a defined OOIP in the Muddy channel sand. However, the effective oil and gas volume in the top layer of the low-permeability sand is being tuned during the history matching to match the decline in reservoir pressure. The main procedures in this approach of history matching are listed below:

- The monthly rate of well oil production was used as the well production control.
- The effective oil and gas volumes in the top layer were adjusted to match the decline in reservoir pressure during the first 5-year production.
- Aquifer size and relative permeabilities were adjusted to match the observed advancing front of water incursion.
- Gas injection volume was adjusted to compensate the difference between the produced gas volume and the simulated gas production before the blow down.

Initial Fluid Distributions. In the simulation model, initial oil, gas, and water distributions are calculated by pressure equilibrium after the fluid contacts and capillary pressure functions have been defined, Figure 18. Simulation models with different gas-oil contact, oil-water contact, and initial fluid distribution settings were tested to match the measured field pressure decline. Some details of the history matching procedure will be discussed below. It was found that the best match came with the model configured with the data provided in Hurd's paper [5]. As a result, the connate water saturation of 6.5% was assumed in the oil zone and gas cap. The original gas-oil contact was set at 675 ft above the sea level and oil-water contact was set at -73 ft below the sea level as shown in Figure 21. A residual oil saturation of 5%, considerably low for a weakly water-wet rock, was used for the water zone below the oil-water contact. The setting of the residual oil saturation in the water zone has almost no effect on the simulation.

Rock Wettability and Relative Permeabilities. Figure 16 shows the spontaneous imbibition rates measured from Grieve Muddy cores by Dr. Xie *et al* [6] at the Chemical & Petroleum Engineering Dept., University of Wyoming. Eight one-inch core plugs, drilled from the cores of four different wells, have been tested. Four of them were drilled from the Facies A intervals and the other four from the Facies B/C intervals. The results from spontaneous imbibition tests indicate that the reservoir rock of the Muddy channel sand in Grieve Field is weakly water-wet. Because no lab-measured relative permeability of Grieve Field is available, relative permeabilities were assumed, Figure 17, based on the residual oil and connate water saturations and the trend of relative permeabilities of mix-wet rocks. To examine the effect of rock wettability on the water incursion from the down-dip aquifer, a series of simulation runs were performed with a water relative permeability changed from very weakly water-wet to very strongly water-wet. It was found that water influx is much more sensitive to aquifer size than the shape of relative permeability curve when the end points of the relative permeability curves were fixed.

Aquifer Size and Water Incursion. The down-dip water zone in the simulation model contains a water volume of 108 million rb below the original oil-water contact. Cells in the water zone are connected to numerical aquifers. To match the observed advancing front of water influx, the total aquifer size was increased to about 700 billion rb of pore-volume water. A hydrostatic equilibrium pressure was initially defined for the aquifer. Ternary views of water incursion are illustrated in Figure 21-23. By the end of July 2006, history matching estimated a net water increase of 20 million rb in the Muddy channel sand, Table 2 and 3.

History Matching of Reservoir Pressure Decline. Different strategies were applied for different production periods to match the reservoir pressure. As shown in Figure 15, the reservoir has endured three distinct periods: the initial depletion before 1962, the period of pressure maintenance by gas injection, and the blow down starting in 1977. During the initial depletion, when no water was produced and water influx was limited, the pressure decline was mainly caused by oil and gas extraction. It was found that the simulated pressure decline was much faster than the measured decline for any of the candidate models if no porosity was defined in the top layer. It implies that the actual reservoir volume is larger than the volume of Muddy channel sand. Consequently, the model with an OOIP of 67 MMSTBO, the largest one among the candidate models, was picked. In addition, an effective porosity of 2% in the top layer has resulted from the history matching in order to retard the pressure decline, which adds an OOIP of 5.55 MMSTBO in the top layer. Matching the actual gas production is found to be difficult, partially because some of the gas production data are missing. When the reservoir pressure was maintained by gas injection, the producing gas-oil ratio became very high from some of the wells. However, the simulation model under oil-rate well control has difficulty to produce enough gas. To match the stabilized pressure in that period, gas injection volume was reduced to compensate the difference between the produced gas volume and the simulated gas production. The simulated net gas production, the total production minus the total injection, is about 63 BCF in comparison to 69 BCF of estimated net gas production. During the blow down well production control was changed to bottom-hole pressure control but with the up-limitation of the actual oil rate. The change in reservoir pressure distribution is illustrated in Figure 18-20. The entire match of the pressure decline is given in Figure 15.

Estimates of OOIP in the Three Regions. Three fluid-in-place regions are defined in the simulation model. They are:

Region 1: the overlain low-permeability sandstone interval (the top layer), above the original oil-water contact
Region 2: the water zone below the original oil-water contact
Region 3: the Muddy channel sand interval above the original oil-water contact

A simulation report from the history matching is given in Table 2 and 3, which shows the estimated initial and current oil, gas, and water in place in each region. In summary, the history matching based on full-field material balance estimates the OOIPs as:

Region 1: 5.55 MMSTBO
Region 2: 3.15 MMSTBO
Region 3: 66.99 MMSTBO

History matching reveals that about one MMSTBO of oil and 8.2 BSCF of gas have moved down from the overlain low-permeability sand interval into the Muddy channel sand interval during reservoir depletion, Figure 24-29. This explains the reason of the inconsistency in OOIPs estimated previously from volumetric and material balance calculations [5] because volumetric estimates are mostly based on the reservoir volume in the Muddy channel sand. As shown in Table 3, it is estimated that about 38 MMSTBO currently remains in the Muddy channel sand and 4.5 MMSTBO in the overlain low-permeability interval.

Simulation Forecasts of CO2 Flooding Performance

In many miscible CO2 flooding field projects, CO2 is injected alternately with water, such as the Lost Soldier and Wertz CO2 miscible floods at Bairoil Dome of Wyoming. The concept of using CO2 WAG (water alternating gas) injection technique is to improve injection profile and reduce gas channeling. However, for reservoirs with large dip angles, gravity segregation of injected CO2 and water might leave a large volume of remaining oil uncontacted with injected CO2 and, consequently, reduce the overall WAG flooding efficiency. It is believed [5] that gravity segregation of solution gas and oil occurred continually within the Grieve Muddy reservoir through the initial 4 to 5 years of production prior to any water being produced. For the stratigraphic/structural trap of Grieve Muddy reservoir which has an average structural dip of 15 degrees, using continuous CO2 injection into the reservoir's gas cap can be much more effective than CO2 WAG injection to recover its remaining oil. The reservoir depth, at 6,900 ft, and oil gravity, 37^{o}API, are considered favorable for miscible gravity stable CO2 flooding. In this study, a compositional Eclipse model was developed to simulate different scenarios of gravity stable CO2 flooding in the Grieve Muddy reservoir, in which the initial pressure and saturation (oil, gas, and water) distributions resulted from the history matching.

Slim Tube MMP Analysis. Miscibility between reservoir oils and injected CO_2 usually develops through a dynamic process of mixing, with component exchange controlled by phase equilibria and local compositional variation along the path of displacement. CO_2 is not miscible on the first contact with reservoir oils. However, with a sufficient high pressure, CO_2 could achieve dynamic miscibility with a reservoir oil in a multiple contact process. The slim tube test has been used for decades as a trusted method for determining minimum miscibility pressures (MMP). Using the well-head oil sample collected from Well No.9, slim tube experiments have been conducted by Dr. Adidharma's group at the Chemical & Petroleum Engineering Dept., University of Wyoming [7]. Under pure CO_2 injection and the Grieve reservoir temperature of 135 ^{o}F, the MMP for the Grieve oil sample is estimated at 2068 psi.

A 9-Component Simulation Model. Copies of the original reports of the gas chromatographic (GC), distillation and differential liberation analysis on one bottom-hole crude sample from Grieve Unit No.1 were obtained from Elk Petroleum. Because oil composition is crucial information needed for defining equation of state (EOS) in compositional simulation, for this study, well-head oil samples from Well No.9 were collected and sent to Western Research Institute (WRI) in Laramie and Core Lab in Houston for additional GC and compositional analysis. The Peng-Robinson EOS was used in the simulation model and the composition of Grieve oil was lumped into nine components. They are CO_2, nitrogen, methane, ethane, propane, lumped component of butanes to benzene, lumped component of heptanes to xylenes, lumped component of nonanes, and lumped component of decanes plus.

Injection/Production Well Configuration. Various scenarios have been simulated with different injection/production well configurations. The number of injection wells was increased from 6 to 10 to achieve a better flooding profile and to increase CO_2 injection volume. Figure 30 shows the locations of the ten injection wells placed at the structure top, named 'Inj12' (Well #12), 'Inj30' (Well #30), 'CO2I1' (Well #50), 'CO2I2' (Well #51), 'CO2I3', 'CO2I4', 'CO2J1', 'CO2J2', 'CO2J3', and 'CO2J4'. Four of them are converted from existing wells, i.e. Well #12, Well #30, Well #50, and Well #51. The rest are new injection wells. Various configurations were simulated to reopen the existing production wells after the reservoir was repressurized. It was found that the most effective way was to produce from the wells at the structure bottom as close as possible to the original oil-water contact. Presented in this report, simulated scenarios include up to 16 production wells. They are Well #17, Well #16, Well #6A, Well #39, Well #2, Well #41, Well #1-22-1, Well #43, Well #44, Well #18, Well #19, Well #32, Well #31, Well #29, and two new wells, 'NEW1' and 'NEW2' as shown in Figure 30.

Reservoir Repressurization and CO2 Injectivity. The current average pressure in Grieve Muddy reservoir, indicated from history matching, is probably between 800 and 900 psi. A bottom-hole pressure of 750 psi measured from Well #9, the only well currently producing, appears consistent with that estimation. To optimize the miscibility between reservoir oils and injected CO_2, the reservoir should be repressurized to above the MMP of 2068 psi before activating any producing well. Because the average formation fracture gradient at Grieve Field is estimated at more than 0.75 psi/ft, the pressure interval between the fracturing pressure and MMP, at a depth of 6900 ft, is sufficient to accommodate a miscible CO2 flooding operation. In the design of simulation scenarios, the reservoir average pressure was targeted between 2100 and 3600 psi during the production phase, as illustrated in Figure 31. In that targeted pressure interval and at the reservoir temperature of 135ºF, CO2 formation factor can vary from 0.54 to 0.42 rb/MCF [8]. Simulation forecasts reveal that an injection of 90 BCF or more of CO2 will be required to repressurize the reservoir. Because injected CO2 at well bottom is most likely to be under supercritical condition, CO2 injection rate at reservoir condition can be estimated as liquid radial flow:

$$q = \frac{2\pi kh(P_{inj} - P_{res})}{1.127\mu \ln(r_e / r_w)}$$

where *q* – injection rate, rb/day; *k* – permeability, darcy; *h* – formation thickness, ft; *Pinj* – bottom-hole injection pressure, psi; *Pres* – reservoir pressure, psi; μ – fluid viscosity, cp; *rw* – wellbore radius; and *re* – distance from the well where the pressure stabilized. It is estimated that wells perforated in the high permeable Muddy channel sand, with an average permeability of 220 md, should be capable of taking more than 5,000 MCF/day of injected CO2 without any well stimulation. In fact, most of Grieve wells have a record of peak production rates over 2,500 reservoir barrels per day, which is roughly equivalent to 5,000 MCF/day of CO2. Gas injection rate in Well #12, at one period, also exceeded 5,000 MCF/day. Different CO2 injection rates ranging from 5,000 to 12,000 MCF/day have been simulated with the maximum BHP set at 3050 psi. Even though no difficulty appeared in the simulation, hydraulic fracturing stimulation might be needed for wells to inject very high volume rates of CO2 if the permeability-feet thickness of the injection interval is not sufficient at the structure top.

Representative Scenarios. More than twenty scenarios have been generated to simulate the gravity stable CO2 flooding in Grieve Muddy reservoir under different CO2 injection schemes and injection/production well configurations. Only three of the simulated scenarios are presented in this report. The selected examples should provide a good understanding of how much a gravity stable CO2 flooding could achieve. The simulated performance of the three scenarios is compared in Figure 32-42 to show field CO2 injection rate, field cumulative CO2 injection, field oil production rate, field cumulative oil production, field gas production rate, field cumulative gas production, field CO2 production rate, field cumulative CO2 production, field water production rate, field cumulative water production, and field average pressure, respectively. Table 4 provides a summary of the three scenarios for a 14-year operation duration. A similar summary is given in Table 5 for a 30-year operation duration. The specified well configuration and injection/production setting for each scenario is given below.

Scenario 1 reflects a low-side case with limited initial CO_2 supply and a minimum volume of total injected CO_2. Using a low injection rate of 5,000 MCF per well per day, CO_2 was injected into ten injection wells placed at the structure top, named 'Inj12', 'Inj30', 'CO2I1', 'CO2I2', 'CO2I3', 'CO2I4', 'CO2J1', 'CO2J2', 'CO2J3', and 'CO2J4' as shown in Figure 30. A maximum BHP of 3050 psi was set for all injection wells. After six years of CO_2 injection, the reservoir was repressurized to an average pressure of 3200 psi. In the following production phase, only three injection wells were used to inject a daily volume of 15,000 MSCF of CO_2 to maintain the reservoir average pressure above MMP. Ten existing wells were opened to produce in the production phase. They are Well #17, Well #16, Well #6A, Well #41, Well #1-22-1, Well #44, Well #18, Well #19, Well #32, and Well #31. A BHP of 2100 psi was set for all production wells. After 6 years of repressurizing the reservoir and 24 years of producing, Scenario 1 could recover about 19.8 MMBO with only about 89 BSCF of CO_2 being produced and reinjected. Scenario 1 requires a relatively low volume of total CO_2 injection estimated about 234.5 BSCF for a 30-year operation duration.

Scenario 2 assumes that initial CO_2 supply will be abundant and a large volume of CO_2 will be injected to achieve higher oil recovery. Using the same injection well configuration of Scenario 1, ten injection wells injected a daily volume of 110,000 MSCF of CO_2 during the repressurization phase. It only took 2.75 years to repressurize the reservoir to an average pressure of 3200 psi. In the following production phase, four injection wells were used to inject a daily volume of 44,000 MSCF of CO_2 to maintain the reservoir pressure and accelerate oil recovery. A total of 14 wells were opened to produce, including a new well at the southeast corner of the reservoir. They are Well #17, Well #16, Well #6A, Well #2, Well #41, Well #1-22-1, Well #43, Well #44, Well #18, Well #19, Well #32, Well #31, Well #29, and ‘NEW1’. BHP control was the same as that used in Scenario 1. It was estimated that about 20 MMBO would be produced within the first 11.25 years of production and only 2.2 MMBO of additional oil would be recovered in the next 16 years of production.

Scenario 3 was used to estimate the ultimate oil recovery from Grieve Muddy reservoir by gravity stable CO_2 flooding. Similar to Scenario 2, ten injection wells injected a daily volume of 110,000 MSCF of CO_2 during the repressurization phase but the injection duration of 2.25 years was 6 months less than the repressurization time used in Scenario 2. Seven injection wells were used to inject a daily volume of 77,000 MSCF of CO_2 during the production phase, in which two new wells, ‘NEW1’ and ‘NEW2’, were added into the production at the southeast corner of the reservoir, Figure 30. In total, 16 production wells were activated in the production phase. They are Well #17, Well #16, Well #6A, Well #39, Well #2, Well #41, Well #1-22-1, Well #43, Well #44, Well #18, Well #19, Well #32, Well #31, Well #29, ‘NEW1’ and ‘NEW2’. BHP control was the same as that used in Scenario 1 and 2. Even thought Scenario 3 injects about 50 % more volume of CO_2 than Scenario 2, Scenario 3 would produce 23.2 MMBO, only one MMBO more than the estimated 22.2 MMBO from Scenario 2 as shown in Table 5.

Oil Recovery and Peak Oil Production Rates. In Scenario 3, it was estimated that more than 23 million barrels of oil could be recovered by gravity stable CO_2 flooding after 30 years of CO_2 injection, Figure 35. The movement of the front oil bank is shown in Figure 43-46. For lower CO_2 injection volumes, Scenario 1 and 2, between 20 and 22 MMBO could still be produced in a 30-year operation. Simulation predicts that about 80% of the recoverable oil would be produced within the first 5 to 6 years of production, Figure 34-35. Without adding any new production well in Scenario 1, simulation predicts a peak production rate of 8,300 STBO/day by opening 10 existing wells. In cases of using high CO_2 injection volumes and producing from 14 or 16 wells, Scenario 2 and 3, daily oil production rate could reach more than 12,300 STBO/day as shown in Figure 34.

Gas and Water Productions. Following the breakthrough of the main oil bank, a large spike in gas production rate was predicted as shown in Figure 36. The maximum daily gas rate could reach as high as 40,000, 109,000, and 170,000 MSCF/day for Scenario 1, Scenario 2, and Scenario 3, respectively. Most of the produced gas is CO_2 and needs to be recycled. A summary of gas and water productions for each scenario are given in Table 4 and 5. As discussed in the previous section, the water relative permeability used in simulating CO_2 flooding reflects a mixed-wet or weakly water-wet reservoir, Figure 17. In all the three scenarios, the cumulative water production was estimated about the same as the total oil production after a 30-year operation, Table 5.

Overall CO_2 Usage. As given in Table 4 and 5, a CO_2 volume ranging from 119 to 161 BCF would have to be purchased for a 14-year operation while about 146 to 188 BCF would be needed for a 30-year operation. The net CO_2 usage efficiency, the ratio between total purchased CO_2 and total produced oil, varies from 7.3 to 8.1 mscf/bo in the simulated cases. However, the volume of CO_2 being produced and reinjected for a 30-year operation could triple the amount of the CO_2 volume recycled in a 14-year operation. The cost for CO_2 separation, re-compression, and re-injection can be an obstacle for using very high volume CO_2 injection during the producing phase. It was predicted that, Figure 47, almost the entire Muddy reservoir would be swept by gravity stable CO_2 flooding.

CO_2 Sequestration Potential At Grieve Field. Because of its unique geologic setting, the Grieve Muddy reservoir is considered a good candidate for a CO_2 sequestration site. For example in Scenario 3, Table 5, about 188 BCF of injected CO_2 could be sequestered at the end of the 30-year operation. Calculated by using an average CO_2 formation volume factor of 0.48 rb/MSCF, 188 BCF of CO_2 is equivalent to about 90 million reservoir barrels, or 60% of the reservoir pore volume in the Muddy channel sand. Because CO_2 is denser than natural gas in the reservoir, some natural gas can be trapped at the structure top above the injection wells as shown in Figure 48-49. Wood *et al* have developed a screening model for line-drive CO_2 flooding [9]. The model predicts oil recovery and CO_2 storage potential based on a set of dimensionless groups that includes the effect of reservoir dip. For comparison, the screening model was used to calculate oil recovery and sequestered CO_2 volume with the parameters from the Grieve field configuration. As shown in Figure 50, the screening model predicts that injected CO_2 may occupy about 60% of total pore volume, regardless of changes in initial oil saturation, which is quite consistent with the simulation prediction. The oil recovery forecasted from the simulation is slightly better than the screening model prediction.

Conclusions and Recommendations

The main results and conclusions drawn from this evaluation are listed below:

1. Because of its unique geologic setting, Grieve Muddy reservoir is evaluated favorable for gravity stable CO_2 flooding and, at the end of flooding operation, the reservoir can also be used as a potential CO_2 sequestration storage.
2. The CO_2-oil minimum miscibility pressures in Grieve Muddy reservoir is estimated at 2068 psi by slim tube analysis.
3. Wettability tests confirm that Grieve Muddy reservoir rock is weakly water-wet.
4. An OOIP estimation of 67 MMBO in Grieve Muddy channel sand and 5.55 MMBO in the overlain low-permeability sandstone interval was resulted from a simulation history matching based on the full-field material balance.
5. 90 BSCF or more of CO_2 would need to be injected to repressurize the reservoir to an operation pressure above the MMP before any production. The repressurization phase could last 2.25 to 6 years depending on CO_2 injection volume rates. The initial CO_2 demand is estimated to be in the 50,000 to 110,000 MSCF/day range.
6. Simulation shows that between 20 and 23 MMBO could be produced by a 30-year operation of CO_2 flooding while about 80% of the recoverable oil would be produced within the first 5 to 6 years of production. Total CO_2 purchased are estimated to be in the 119 to 188 BSCF range depending on the operation duration and CO_2 injection rate. The net CO_2 usage efficiency varies from 7.3 to 8.1 MSCF/BO in the simulated cases.
7. The reservoir has potential to sequester more than 145 BSCF of CO_2 at the end of a gravity stable CO_2 flooding operation.

There are several issues that are identified and recommended for further refining the simulation evaluation in any subsequent study.

1. A better geologic description of the aquifer system that supplies the down-dip water zone of Grieve Muddy reservoir will help to define more realistic aquifer size and connection in a simulation model. The communication between Grieve Muddy channel sand and the underlying Cloverly formation is not well understood and needs to be reviewed.
2. Lab-measured oil-water and gas-oil relative permeabilities provide an important base reference in history matching, which are currently not available.
3. Obtaining field-measured residual oil saturation from near-wellbore tracer tests is highly recommended. The measured saturation data can be used to verify the OOIP estimation or provide an adjusted estimation.
4. Because of the time restriction, well-by-well history matching has not been performed in this study. A good match at well-level could provide a better estimation of current fluid distribution but would not likely result in any significant change to current fluid-in-place estimated from a full-field material balance.

References

1. DeJarnett, B.B.: “Stratigraphic Core Study of the Muddy Formation”, a report of a work performed for the Grieve Field Study, August, 2007.
2. Yin, P.: “Diagenesis of Muddy Sandstones”, a report of a work performed for the Grieve Field Study, August, 2007.
3. Lawson, D.E.: “Geology of the Grieve Field, Natrona County, Wyoming”, Wyoming Geological Assoc. Guidebook, 17th Ann. Field Conf., p. 284-292, 1962.
4. Mitchell, G.: “Grieve Oil Field, A lower Cretaceous estuarine deposit”, Wyoming Geological Assoc. Guidebook, 30th Ann. Field Conf., p. 147-165, 1978.
5. Hurd, J.D.: “Grieve Unit – High Recovery Muddy Sand”, SPE 2905, 1970.
6. Xie, X. and Wang, W.: “Wettability Study of Muddy Sandstone from Grieve Field”, a report of a work performed for the Grieve Field Study, October, 2007.
7. Adidharma, H: “Determination of CO2-Oil Minimum Miscibility Pressures for Grieve and Austin Creek Oil Samples from Slim Tube Experiments”, a report of a work performed for the Grieve Field Study, June, 2007.
8. Jarrell, P.M., Fox, C.E., Stein, M.H. and Webb, S.L.: “Practical Aspects of CO2 Flooding”, SPE Monograph Volume 22, Henry L. Doherty Series, 2002.
9. Wood, D.J., Lake, L.W.SPE, and Johns, R.T.: “A Screening Model for CO2 Flooding and Storage in Gulf Coast Reservoirs Based on Dimensionless Groups”, SPE 100021, 2006.

Table 1. Well tops of facies and calculated average porosity and permeability by facies in Grieve Muddy reservoir.

Well_No	WELLAPI	elevKB	SS_top	C_top	B_top	A_top	A_base	SS_Perm	C_Perm	B_Perm	A_Perm	SS_Por	C_Por	B_Por	A_Por
39	4902505432	6732	6612	6647.74	6659.86	6683.62	6724.16								
11	4902505431	6791	6421	6465.59	6494	6502	6528		125.333	204.625	376.25		21.7667	23.7625	25.24
14	4902505434	6789	6293.31	6329.75	6342	6342	6342								
6A	4902505435	6710	6540	6581.8	6589.72	6621.41	6675.93								
16	4902505436	6727	6682.44	6724.31	6744.24	6779.1	6819.93			143.523	431.765			18.3355	22.8529
17	4902505437	6742	6610	6655.53	6670	6674	6674		8.92857	11.55			12.8286	13.05	
40	4902509678	7063	5548	5591	5591	5591	5591								
51	4902522915	7290	6058	6132	6132	6132	6132								
12	4902505424	7061	6138	6181.51	6191.17	6201.84	6231.82		18.9667	26.7	218.529		18.1444	18.29	23.6706
9	4902505427	6873	6416	6464.79	6479.7	6513.72	6537.95			87.4615	561.791			19.9231	24.013
18	4902505407	7018	6872.51	6913.35	6924.54	6934.93	6973.69			9.52222	705.2			14.6333	19.8231
5	4902505408	7186	6854	6893.95	6906.15	6917.84	6933.08			94	545.273			20.025	21.0818
13	4902505410	7165	6653.72	6691.01	6709.25	6719.88	6735.59				313.5				23.85
44	4902505416	7067	6930	6972.49	6986.21	7005.02	7031.95			34.4127				14.2818	
4	4902505417	7134	6868	6907.95	6916.08	6938.95	6959.28		9.36667	170.182	476.211		15.4	20.6045	21.7474
10	4902505419	6986	6530	6569.95	6580.12	6600.95	6631.95			183	246.261			24.44	25.7522
15	4902505420	7092	7090.19	7131.97	7141.57	7161.27	7189.56			28.9126	253.65			16.1526	20.14
7	4902505422	7125	6515	6549.36	6570.71	6578.33	6622.54			29.95	219.647			18.05	21.8463
43	4902505423	7080	6995	7027.33	7045.62	7067.99	7095.43				313.6				18.5333
1-22-1	4902505425	6886	6669.14	6708.54	6722.76	6742.56	6777.6			122.4	196.643			19.54	21.7893
41	4902505428	6840	6710	6754.59	6790	6795.13	6818.9		60.0167	257.833	361.5		13.0111	20.5	20.55
2	4902505429	6857	6620.8	6661.59	6675.07	6705.76	6729.47			399.515	1007.5			16.0667	21.9125
8A	4902505430	6825	6826.98	6873.9	6899	6927.02	6972.22		17.8143	140.75	161.391		12.6571	18.2821	19.6698
26-8	4902505387	7118	6979	7053	7075	7079	7079		4.19421	0.1			12.6105	9.425	
23	4902505388	7294	6850.87	6904.89	6926.17	6963.81	6963.81		6.35	10.0865			11.35	14.9703	
29	4902505391	7324	7145	7205	7222	7235	7270		26.7182	165.25			16.4941	19.7125	
22	4902505395	7328	6913	6973	6999	7008	7020		33.3042	255.222	386.417		14.1808	20.6333	21.6583
31	4902505397	7119	7048	7104	7118	7134	7150	0.1	18.8543	213.063	258.875	9.5	15.9357	20.3188	19.9812
21	4902505398	7342	6835.09	6874.8	6886.41	6914.85	6952.24			2.625	261.608			14.05	19.2184
32	4902505400	7134	7074	7130	7144	7152	7161	0.1	13.1946	161.75	470.75	3.9	14.8	18.3875	20.5875
19	4902505402	7166	6962.45	7005.05	7019.16	7042.91	7050.97			73.6235	292.75			15.4471	18.5875
50	4902522633	7341	6411	6446	6468	6484	6508								
42	4902505392	7343	6003	6083	6097	6099	6104	8.816	10.7475			14.04	14.5		
30	4902505394	7342	6548	6611	6631	6631	6635								
20	4902505401	7229	6825	6864.99	6878	6899.66	6917		0.1	74.1773	371.875		11.3	16.9182	21.475
49	4902522592	7349	6479	6526	6536	6558	6566								
MUSTANG-1	4902521889	7363	5862.73	5983.72	5983.72	5983.72	5983.72								
48	4902521776	7337	6668	6699.75	6728.95	6745.98	6791.23								
1-34	4902520833	7183	5744	5791	5791	5791	5791								
24	4902505384	7031	6596	6645	6645	6645	6645	0.30667				12.1067			

Table 2. Estimated initial oil, gas, and water in place in Grieve Muddy reservoir.

Grieve Muddy Reservoir, Simulation Report
1 APR 1954

FIELD TOTALS
PAV = 2906.99 PSIA
PORV= 279013180. RB
(PRESSURE IS WEIGHTED BY HYDROCARBON PORE VOLUME:
PORE VOLUMES ARE TAKEN AT REFERENCE CONDITIONS)

	OIL STB LIQUID	OIL STB VAPOUR	OIL STB TOTAL	WAT STB TOTAL	GAS MSCF FREE	GAS MSCF DISSOLVED	GAS MSCF TOTAL
CURRENTLY IN PLACE	75696192.		75696192.	144015968.	41234605.	54813620.	96048225.
OUTFLOW THROUGH WELLS			0.	0.			0.
WELL MATERIAL BAL. ERROR			0.	0.			0.
FIELD MATERIAL BAL. ERROR			0.	0.			0.
ORIGINALLY IN PLACE	75696192.		75696192.	144015968.	41234605.	54813620.	96048225.

FIPNUM REPORT REGION 1
PAV = 2848.15 PSIA
PORV= 17062248. RB

	OIL STB LIQUID	OIL STB VAPOUR	OIL STB TOTAL	WAT STB TOTAL	GAS MSCF FREE	GAS MSCF DISSOLVED	GAS MSCF TOTAL
CURRENTLY IN PLACE	5553952.		5553952.	2374599.	8663345.	4037585.	12700931.
OUTFLOW TO OTHER REGIONS	0.		0.	0.	0.	0.	0.
OUTFLOW THROUGH WELLS			0.	0.			0.
MATERIAL BALANCE ERROR.			0.	0.			0.
ORIGINALLY IN PLACE	5553952.		5553952.	2374599.	8663345.	4037585.	12700931.

FIPNUM REPORT REGION 2
PAV = 3207.16 PSIA
PORV= 112732633. RB

	OIL STB LIQUID	OIL STB VAPOUR	OIL STB TOTAL	WAT STB TOTAL	GAS MSCF FREE	GAS MSCF DISSOLVED	GAS MSCF TOTAL
CURRENTLY IN PLACE	3147104.		3147104.	108071036.	0.	2273940.	2273940.
OUTFLOW TO OTHER REGIONS	0.		0.	0.	0.	0.	0.
OUTFLOW THROUGH WELLS			0.	0.			0.
MATERIAL BALANCE ERROR.			0.	0.			0.
ORIGINALLY IN PLACE	3147104.		3147104.	108071036.	0.	2273940.	2273940.

FIPNUM REPORT REGION 3
PAV = 2903.78 PSIA
PORV= 149218298. RB

	OIL STB LIQUID	OIL STB VAPOUR	OIL STB TOTAL	WAT STB TOTAL	GAS MSCF FREE	GAS MSCF DISSOLVED	GAS MSCF TOTAL
CURRENTLY IN PLACE	66995136.		66995136.	33570332.	32571260.	48502095.	81073355.
OUTFLOW TO OTHER REGIONS	0.		0.	0.	0.	0.	0.
OUTFLOW THROUGH WELLS			0.	0.			0.
MATERIAL BALANCE ERROR.			0.	0.			0.
ORIGINALLY IN PLACE	66995136.		66995136.	33570332.	32571260.	48502095.	81073355.

Table 3. Simulated current oil, gas, and water in place in Grieve Muddy reservoir, by July 2006.

```
***************************************************
* Grieve Muddy Reservoir, Simulation Report       *
* 20 JLY 2006                                     *
***************************************************
```

FIELD TOTALS
PAV = 894.98 PSIA
PORV= 279013180. RB
(PRESSURE IS WEIGHTED BY HYDROCARBON PORE VOLUME:
PORE VOLUMES ARE TAKEN AT REFERENCE CONDITIONS):

	OIL STB LIQUID	OIL STB VAPOUR	OIL STB TOTAL	WAT STB TOTAL	GAS MSCF FREE	GAS MSCF DISSOLVED	GAS MSCF TOTAL
CURRENTLY IN PLACE	46218765.		46218765.	160585943.	23155165.	10089264.	33244429.
OUTFLOW THROUGH WELLS			29477910.	-16569932.			62803620.
WELL MATERIAL BAL. ERROR			0.	0.			0.
FIELD MATERIAL BAL. ERROR			-483.	-44.			175.
ORIGINALLY IN PLACE	75696192.		75696192.	144015968.	41234605.	54813620.	96048225.

FIPNUM REPORT REGION 1
PAV = 865.54 PSIA
PORV= 17062248. RB

	OIL STB LIQUID	OIL STB VAPOUR	OIL STB TOTAL	WAT STB TOTAL	GAS MSCF FREE	GAS MSCF DISSOLVED	GAS MSCF TOTAL
CURRENTLY IN PLACE	4511268.		4511268.	2536479.	3303833.	974078.	4277910.
OUTFLOW TO OTHER REGIONS	1006887.		1006887.	-161862.	7023081.	1200953.	8224035.
OUTFLOW THROUGH WELLS			35795.	2.			198962.
MATERIAL BALANCE ERROR.			3.	-20.			24.
ORIGINALLY IN PLACE	5553952.		5553952.	2374599.	8663345.	4037585.	12700931.
OUTFLOW TO REGION 2	-2065.		-2065.	-336052.	-8765.	304.	-8461.
OUTFLOW TO REGION 3	1008952.		1008952.	174190.	7031846.	1200650.	8232495.

FIPNUM REPORT REGION 2
PAV = 1210.87 PSIA
PORV= 112732633. RB

	OIL STB LIQUID	OIL STB VAPOUR	OIL STB TOTAL	WAT STB TOTAL	GAS MSCF FREE	GAS MSCF DISSOLVED	GAS MSCF TOTAL
CURRENTLY IN PLACE	3145741.		3145741.	104697866.	1339024.	926570.	2265594.
OUTFLOW TO OTHER REGIONS	1364.		1364.	20749604.	9526.	-1179.	8347.
OUTFLOW THROUGH WELLS			0.	-17376348.			0.
MATERIAL BALANCE ERROR.			-1.	-86.			0.
ORIGINALLY IN PLACE	3147104.		3147104.	108071036.	0.	2273940.	2273940.
OUTFLOW TO REGION 1	2065.		2065.	336052.	8765.	-304.	8461.
OUTFLOW TO REGION 3	-701.		-701.	20413552.	761.	-876.	-114.

FIPNUM REPORT REGION 3
PAV = 878.75 PSIA
PORV= 149218298. RB

	OIL STB LIQUID	OIL STB VAPOUR	OIL STB TOTAL	WAT STB TOTAL	GAS MSCF FREE	GAS MSCF DISSOLVED	GAS MSCF TOTAL
CURRENTLY IN PLACE	38561757.		38561757.	53351598.	18512309.	8188616.	26700925.
OUTFLOW TO OTHER REGIONS	-1008251.		-1008251.	-20587742.	-7032607.	-1199774.	-8232381.
OUTFLOW THROUGH WELLS			29442115.	806415.			62604659.
MATERIAL BALANCE ERROR.			-485.	62.			152.
ORIGINALLY IN PLACE	66995136.		66995136.	33570332.	32571260.	48502095.	81073355.
OUTFLOW TO REGION 1	-1008952.		-1008952.	-174190.	-7031846.	-1200650.	-8232495.
OUTFLOW TO REGION 2	701.		701.	-20413552.	-761.	876.	114.

Table 4. Summary of simulated scenarios under 14-year operation duration of gravity stable CO_2 flooding in Grieve Muddy reservoir.

Grieve Muddy Reservoir Scenario Summary, 14-year Operation Duration

	Scenario 1	Scenario 2	Scenario 3
Targeted Oil in Place, MMSTBO	37	37	37
Repressurization Phase			
CO2 injection wells	10	10	10
Per-well CO2 injection rate, mscf/day	5,000	11,000	11,000
Total CO2 injection rate, mscf/day	50,000	110,000	110,000
CO2 volume factor, rb/mscf	0.42 - 0.54	0.42 - 0.54	0.42 - 0.54
Total CO2 injected, bscf	109.5	110.4	90
Injected CO2 slug size, PORV	0.35	0.35	0.29
CO2 injection duration, years	6	2.75	2.25
Production Phase			
CO2 injection wells	3	4	7
Per-well CO2 injection rate, mscf/day	5,000	11,000	11,000
Total CO2 injection rate, mscf/day	15,000	44,000	77,000
CO2 volume factor, rb/mscf	0.42 - 0.54	0.42 - 0.54	0.42 - 0.54
Total CO2 injected, bscf	37.5	164.1	322.7
Injected CO2 slug size, PORV	0.12	0.52	1.03
Production wells	10	14	16
Total oil produced, mmbo	**15.15**	**20**	**21.4**
Maximum daily oil rate, stbo/day	8,300	12,380	13,600
Total gas produced (including CO2), bscf	37.3	149.4	279.7
Maximum daily gas rate, mscf/day	40,000	109,000	170,000
Total water produced, mmbw	12.9	16.4	18.2
Maximum daily water rate, bw/day	11,600	14,500	16,800
Injection/production duration, years	8	11.25	11.75
Overall CO2 Usage of Both Phases			
CO2 injected, bscf	147	274.5	412.7
CO2 produced & reinjected, bscf	28.1	128.5	251.7
CO2 purchased, bscf	118.9	146	161
Net CO2 utility, mscf/bo	7.84	7.3	7.5
Overall Operation Duration, years	14	14	14

Table 5. Summary of simulated scenarios under 30-year operation duration of gravity stable CO_2 flooding in Grieve Muddy reservoir.

Grieve Muddy Reservoir Scenario Summary, 30-year Operation Duration

	Scenario 1	Scenario 2	Scenario 3
Targeted Oil in Place, MMSTBO	37	37	37
Repressurization Phase			
CO2 injection wells	10	10	10
Per-well CO2 injection rate, mscf/day	5,000	11,000	11,000
Total CO2 injection rate, mscf/day	50,000	110,000	110,000
CO2 volume factor, rb/mscf	0.42 - 0.54	0.42 - 0.54	0.42 - 0.54
Total CO2 injected, bscf	109.5	110.4	90
Injected CO2 slug size, PORV	0.35	0.35	0.29
CO2 injection duration, years	6	2.75	2.25
Production Phase			
CO2 injection wells	3	4	7
Per-well CO2 injection rate, mscf/day	5,000	11,000	11,000
Total CO2 injection rate, mscf/day	15,000	44,000	77,000
CO2 volume factor, rb/mscf	0.42 - 0.54	0.42 - 0.54	0.42 - 0.54
Total CO2 injected, bscf	125	421.1	772.4
Injected CO2 slug size, PORV	0.4	1.35	2.47
Production wells	10	14	16
Total oil produced, mmbo	**19.8**	**22.2**	**23.2**
Maximum daily oil rate, stbo/day	8,300	12,380	13,600
Total gas produced (including CO2), bscf	107.7	392.5	717.2
Maximum daily gas rate, mscf/day	40,000	109,000	170,000
Total water produced, mmbw	19.2	22.1	23.2
Maximum daily water rate, bw/day	11,600	14,500	16,800
Injection/production duration, years	24	27.25	27.75
Overall CO2 Usage of Both Phases			
CO2 injected, bscf	234.5	531.5	862.4
CO2 produced & reinjected, bscf	89	360.8	674.5
CO2 purchased, bscf	145.5	170.7	187.9
Net CO2 utility, mscf/bo	7.35	7.69	8.1
Overall Operation Duration, years	30	30	30

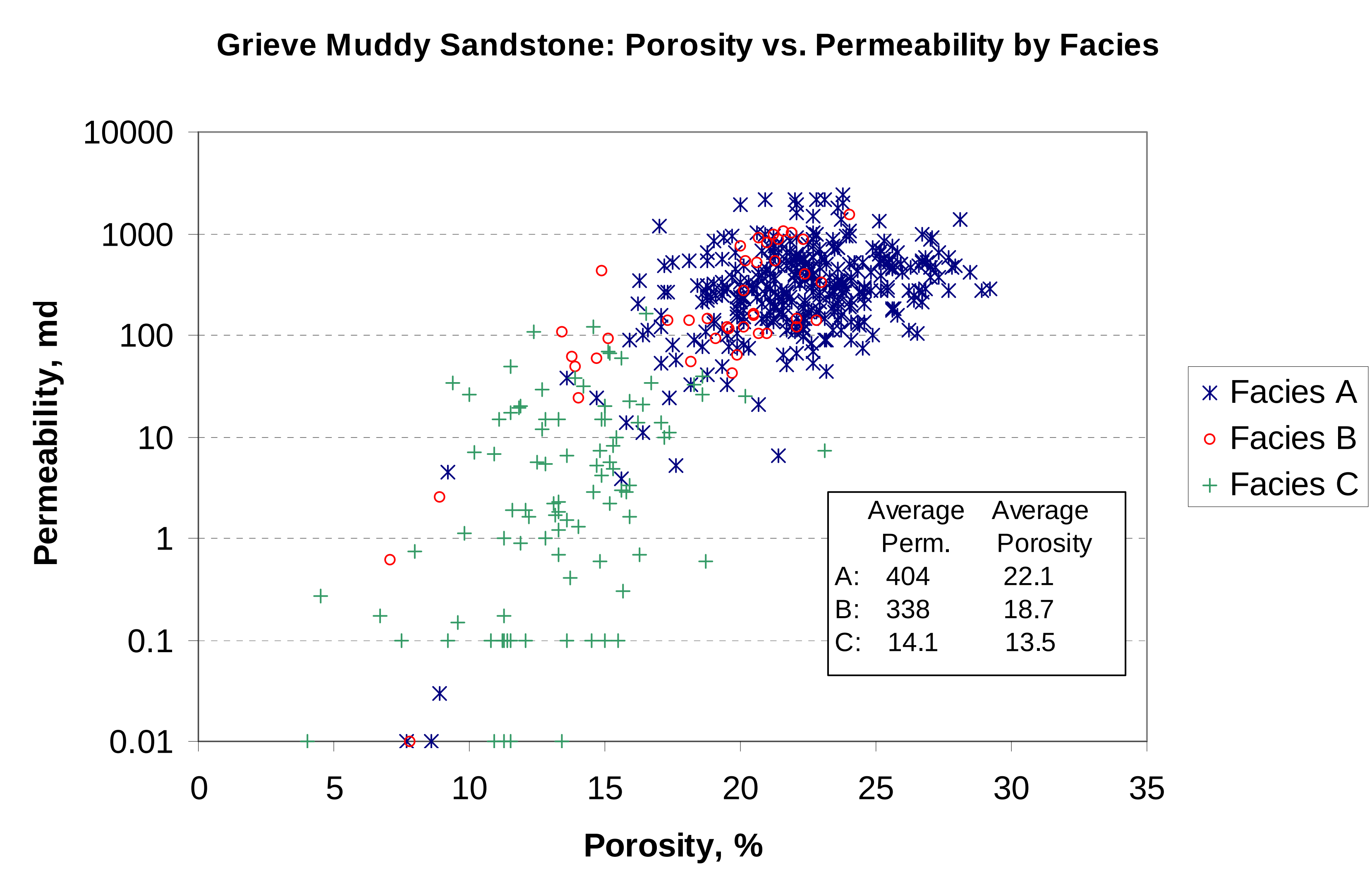

Figure 1. Measured core porosity and permeability by facies in the Grieve Muddy channel sand interval.

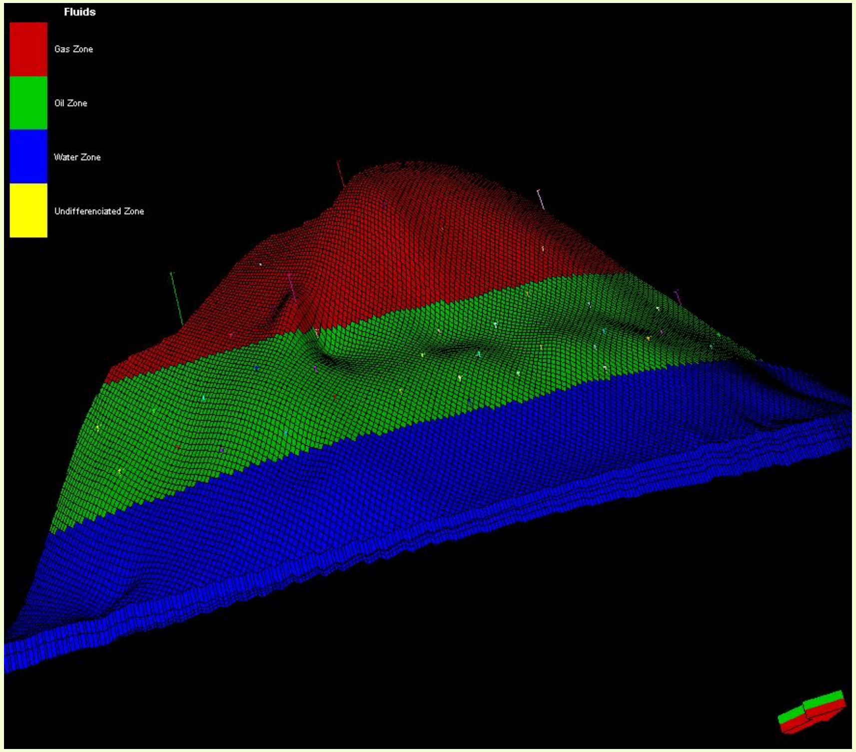

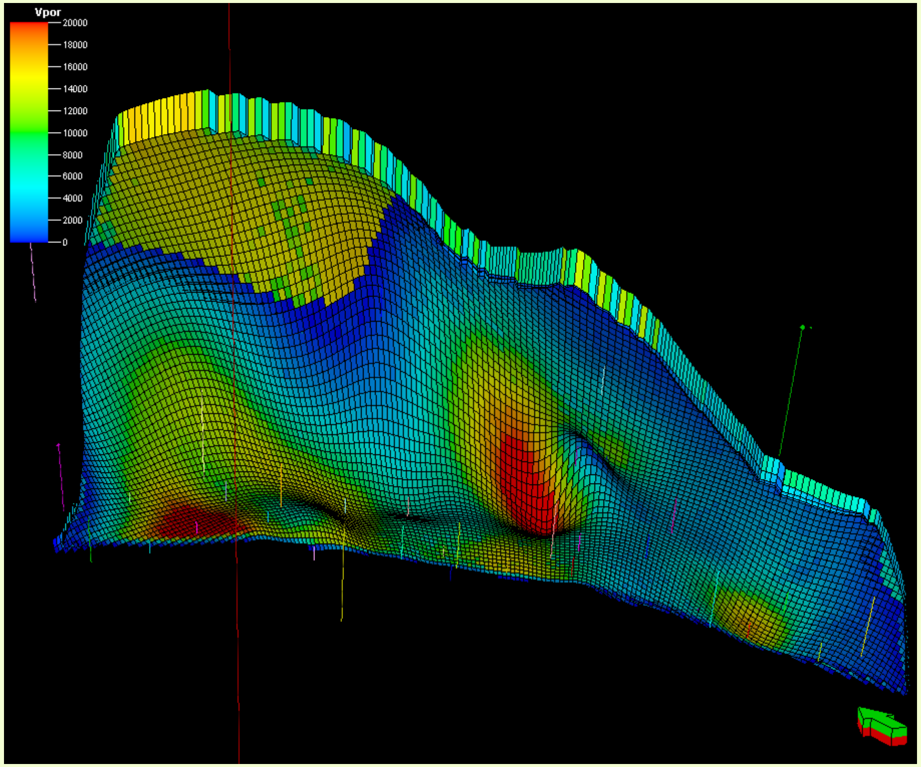

Figure 2. A 3D view of original fluid distributions where the gas-oil contact is set at 675 ft above the sea level and oil-water contact is set at -73 ft below the sea level.

Figure 3. A bottom view of the grid pore volume distribution above the oil-water contact.

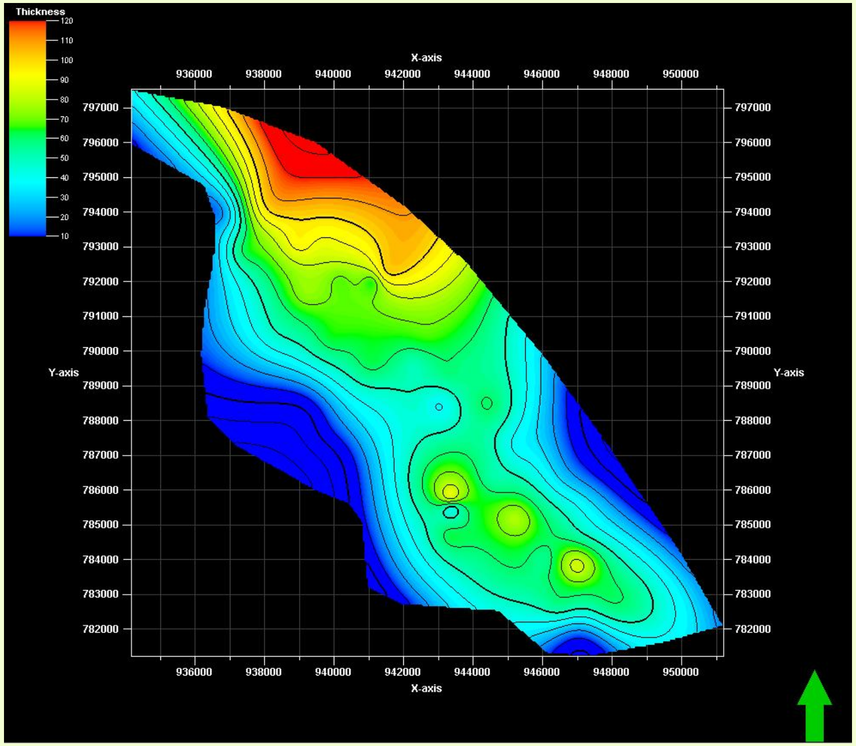

Figure 4. The isochore map of Grieve Muddy channel sand consisting of Facies A, B, and C.

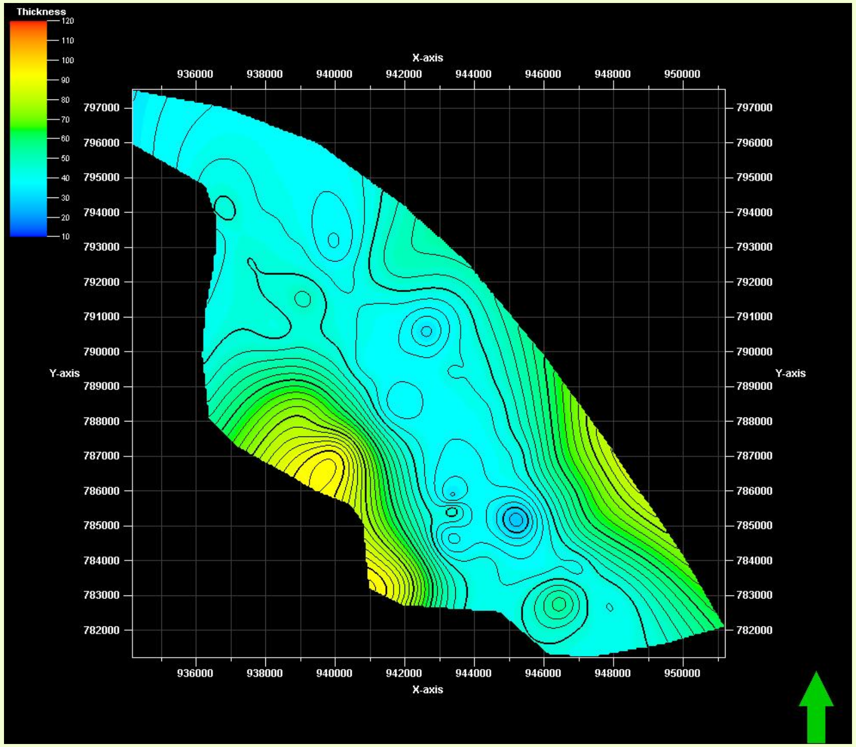

Figure 5. The isochore map of the top layer consisting of Facies D and E.

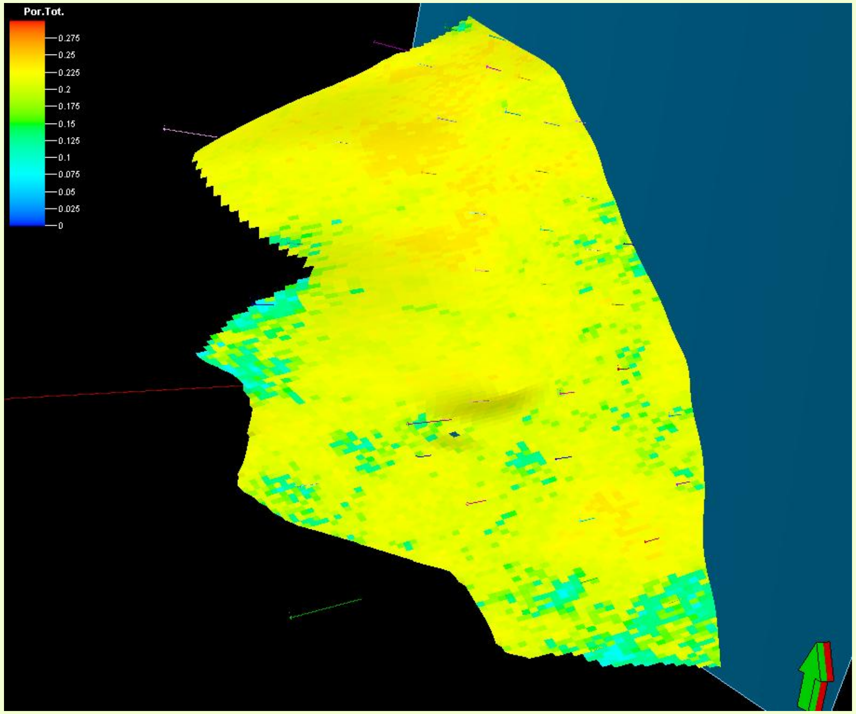

Figure 6. Porosity distribution of Facies A (layer 4) above the oil-water contact.

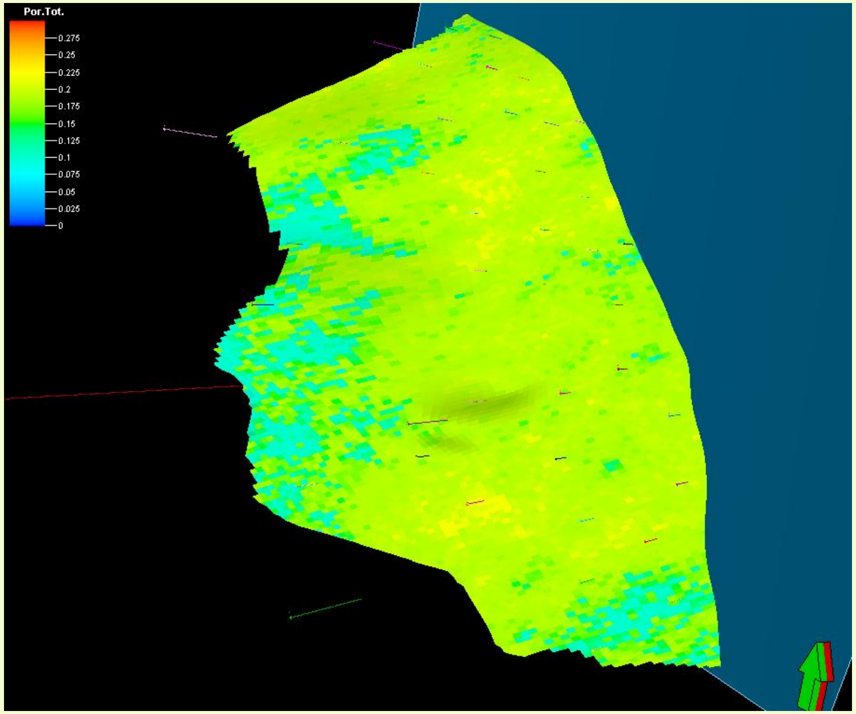

Figure 7. Porosity distribution of Facies B (layer 3) above the oil-water contact.

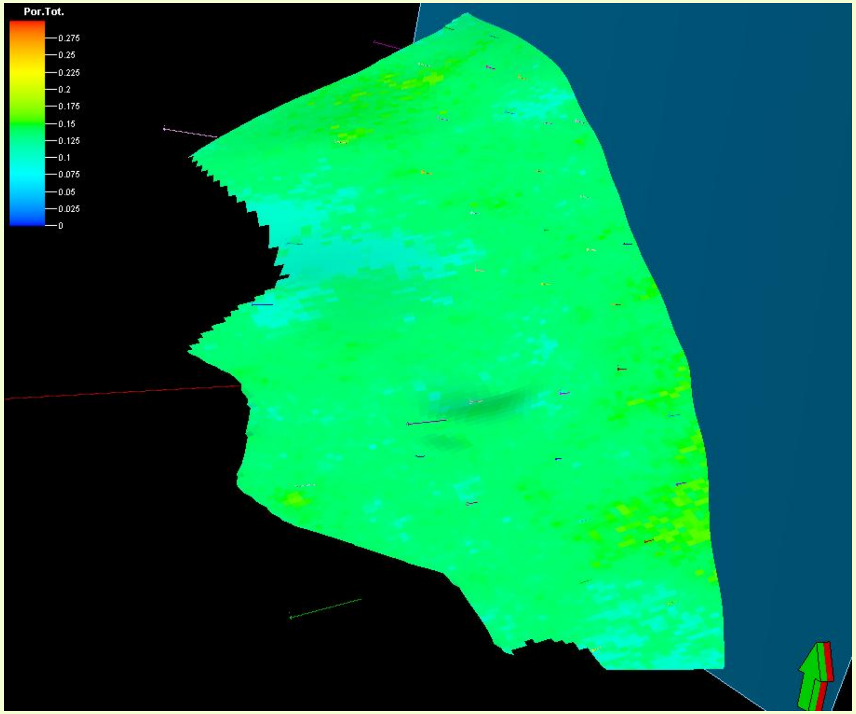

Figure 8. Porosity distribution of Facies C (layer 2) above the oil-water contact.

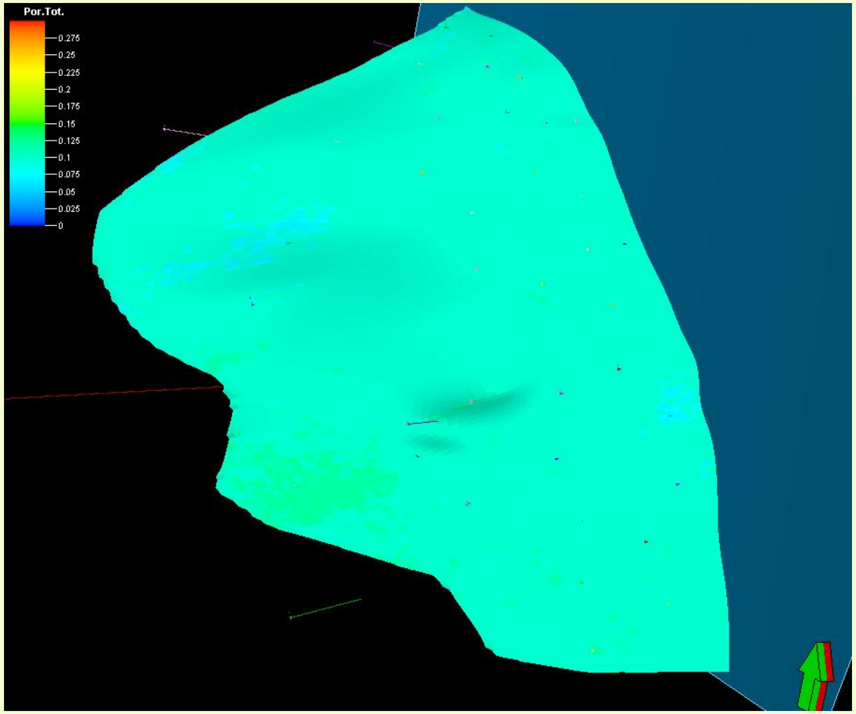

Figure 9. Porosity distribution in the top layer above the oil-water contact.

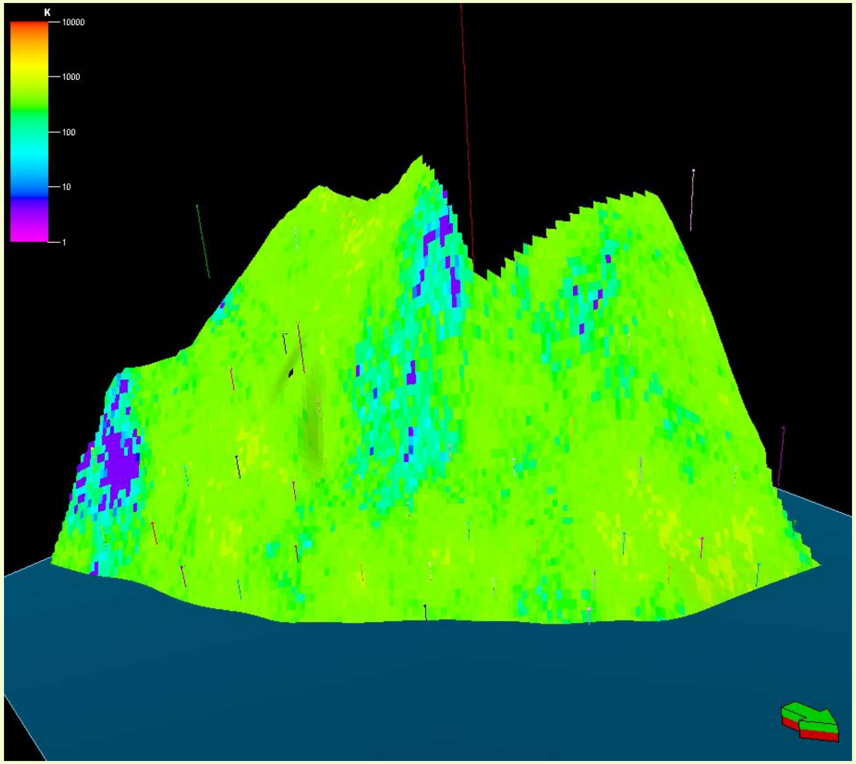

Figure 10. Permeability distribution of Facies A (layer 4) above the oil-water contact.

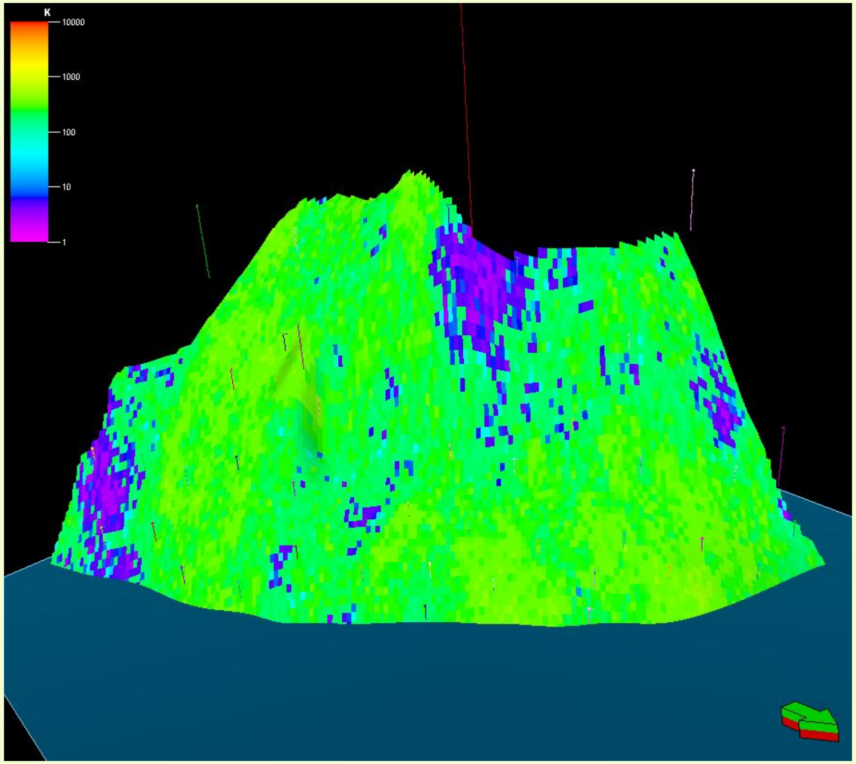

Figure 11. Permeability distribution of Facies B (layer 3) above the oil-water contact.

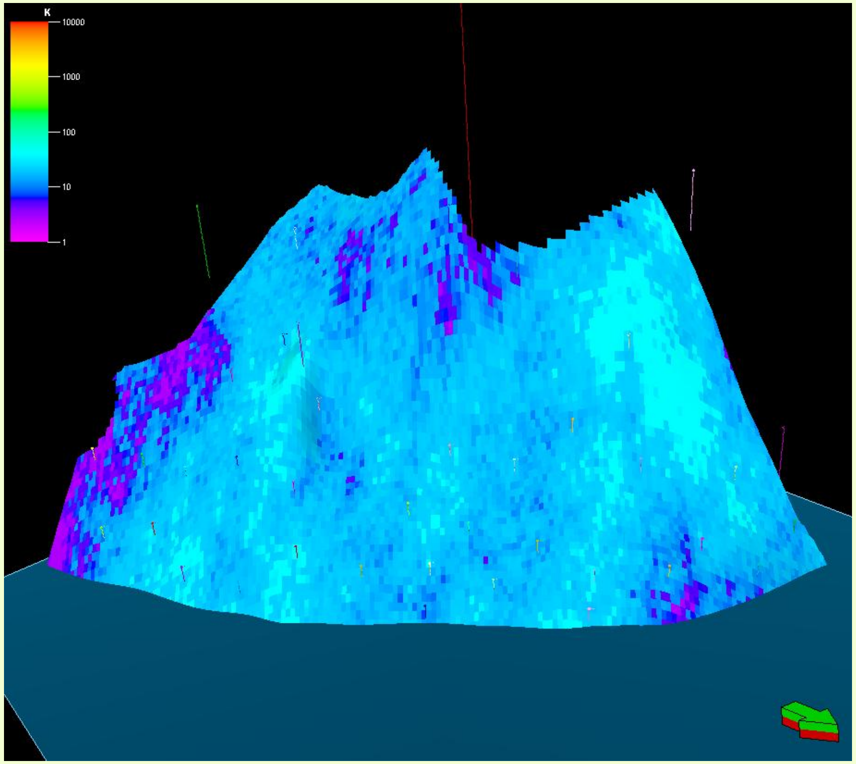

Figure 12. Permeability distribution of Facies C (layer 2) above the oil-water contact.

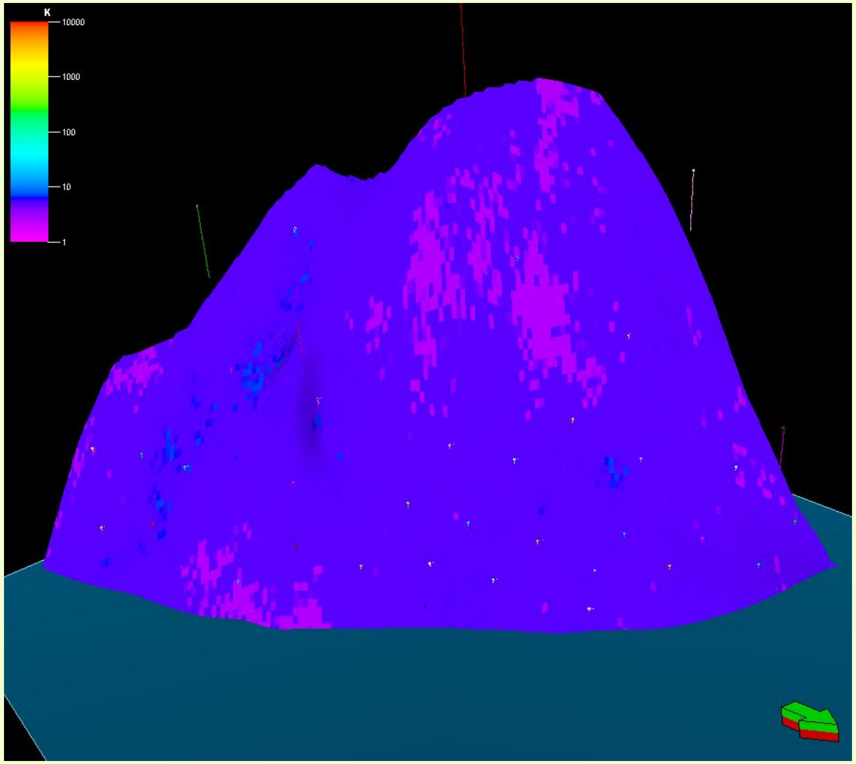

Figure 13. Permeability distribution in the top layer above the oil-water contact.

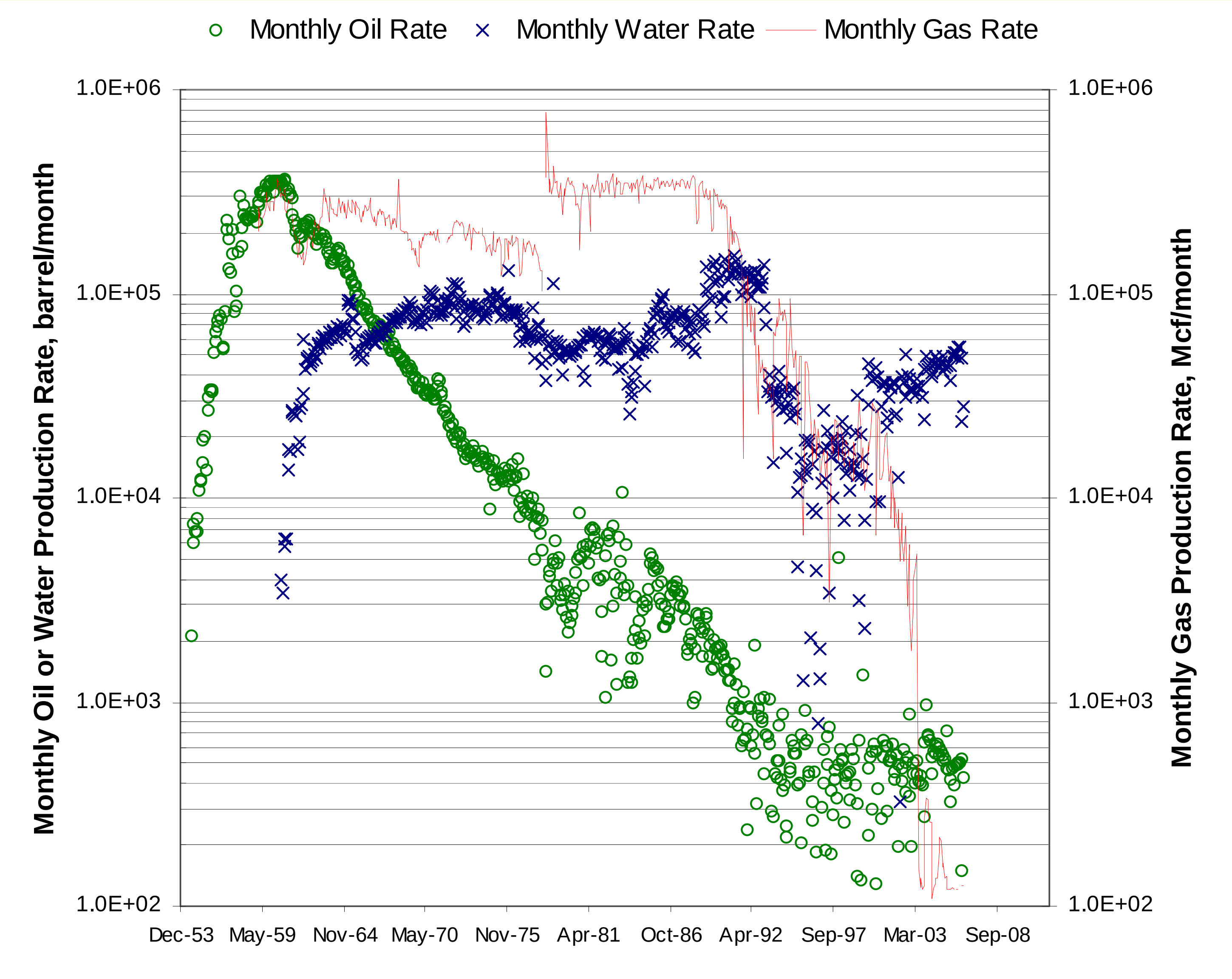

Figure 14. Grieve field monthly oil, gas, and water productions.

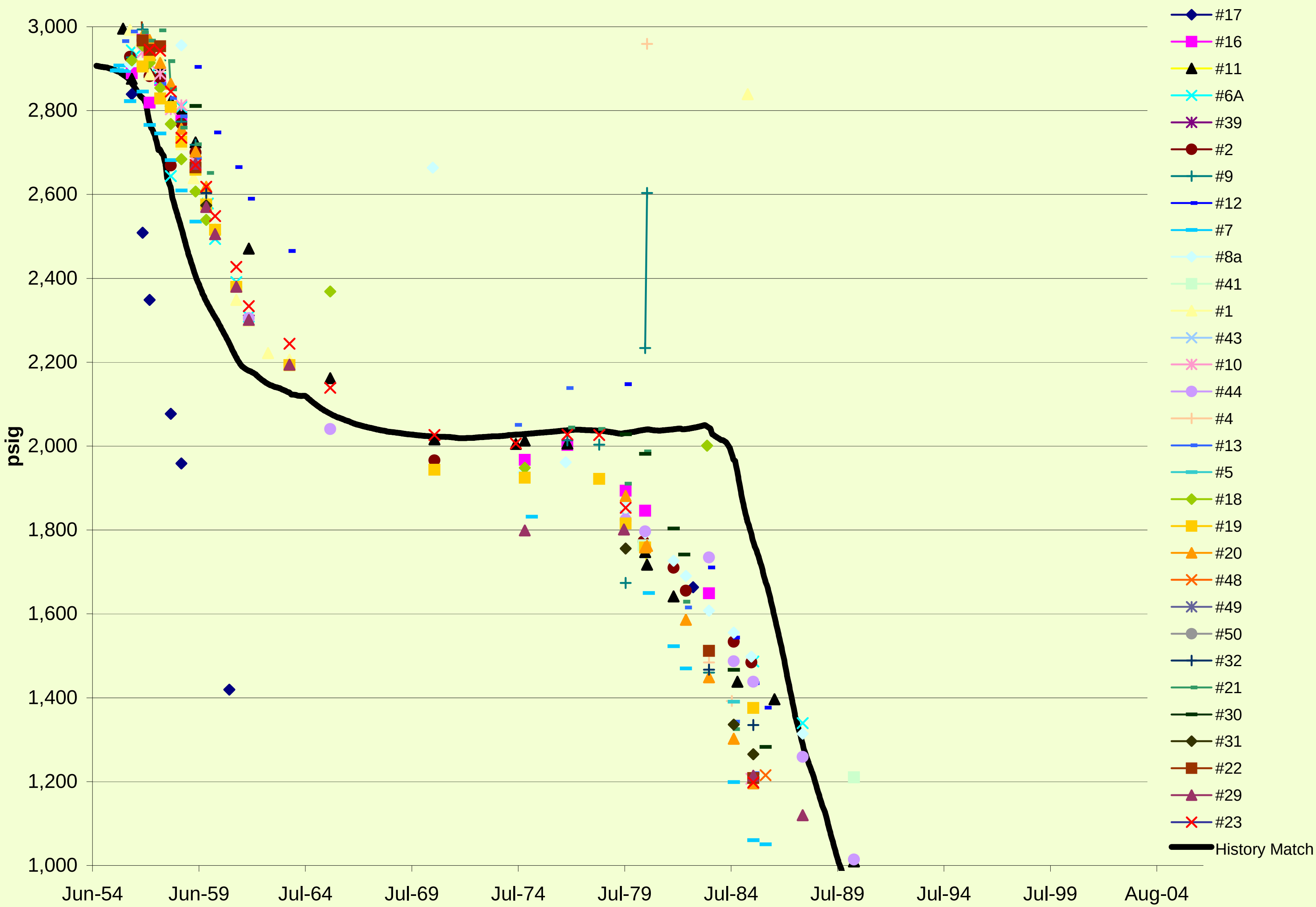

Figure 15. Well bottom-hole pressures measured from pressure build-up tests in comparison with history matched reservoir average pressure.

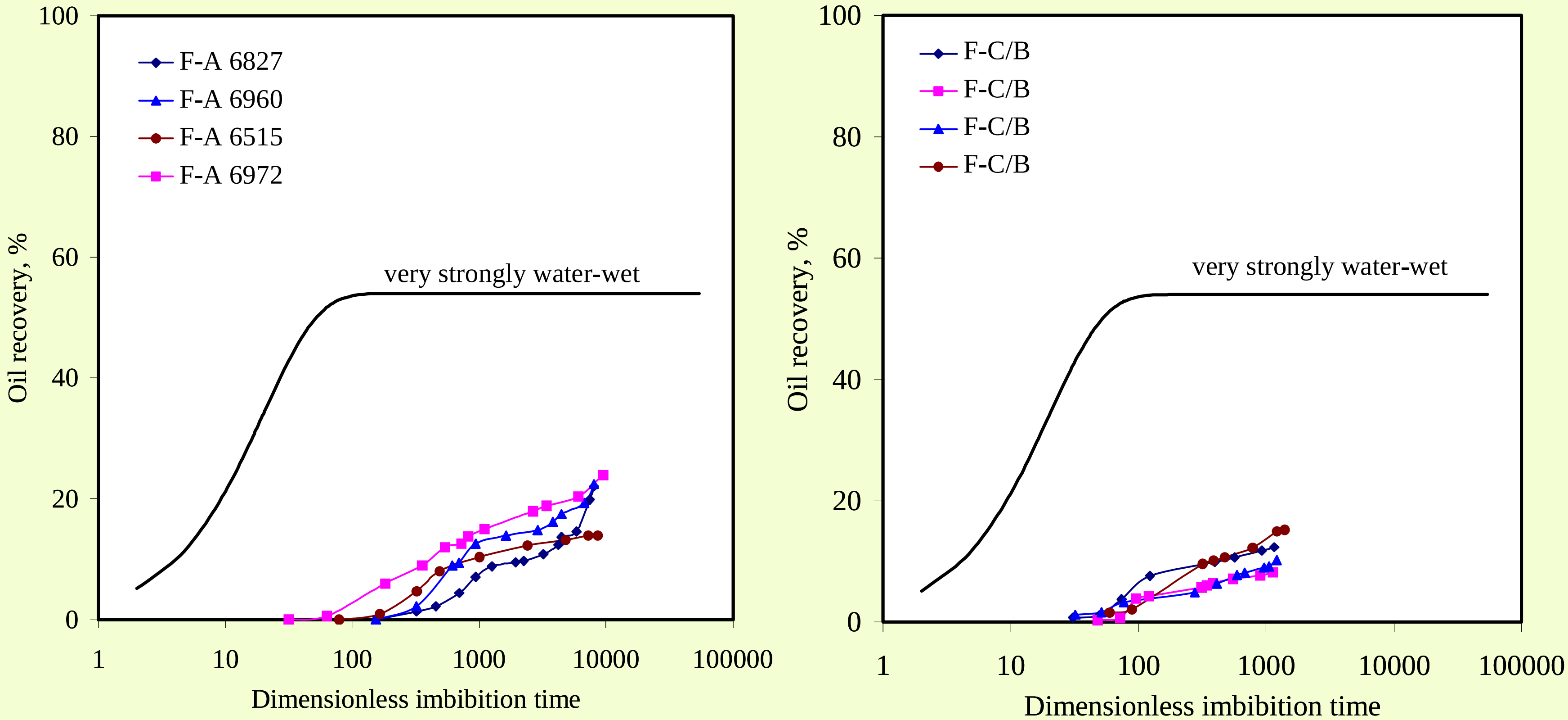

Figure 16. Spontaneous imbibition rates measured from Grieve Muddy cores of Facies A (right) and cores of Facies B/C (left). Copied from the wettability study report by Xie *et al*.

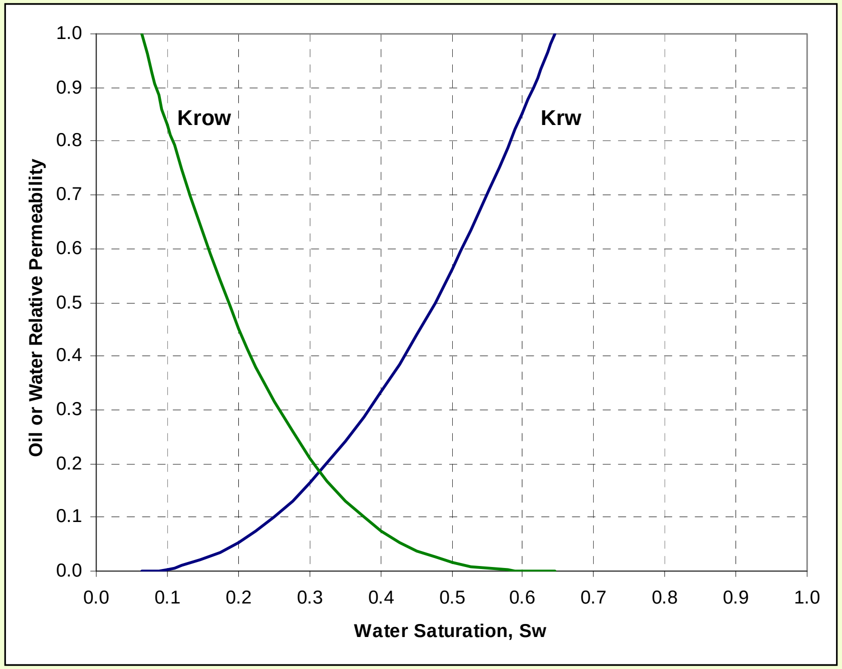

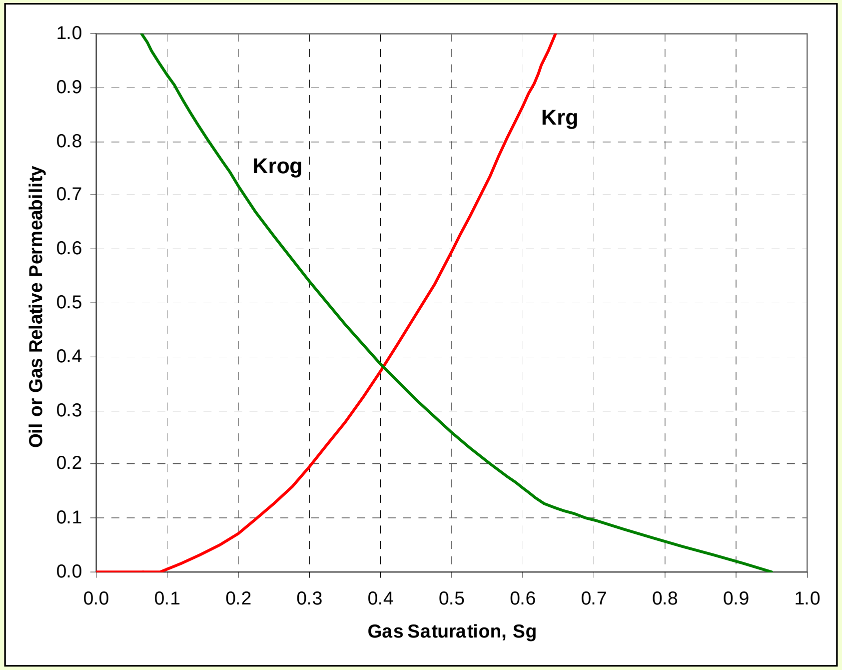

Figure 17. Water-oil relative permeabilities (left) and oil-gas relative permeabilities (right) used in the simulation for Grieve Muddy reservoir.

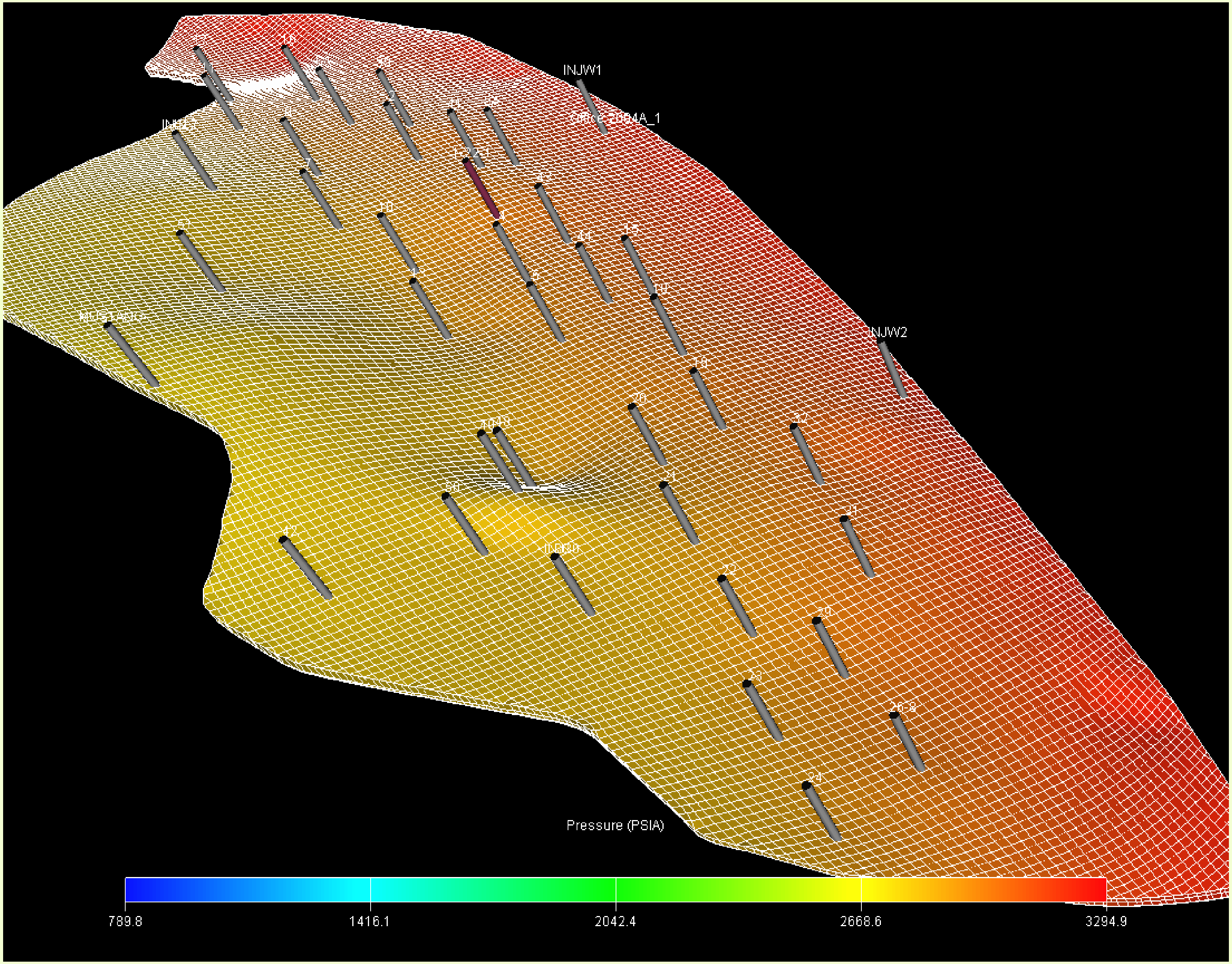

Figure 18. Simulation grids and initial reservoir pressure distribution in August 1954.

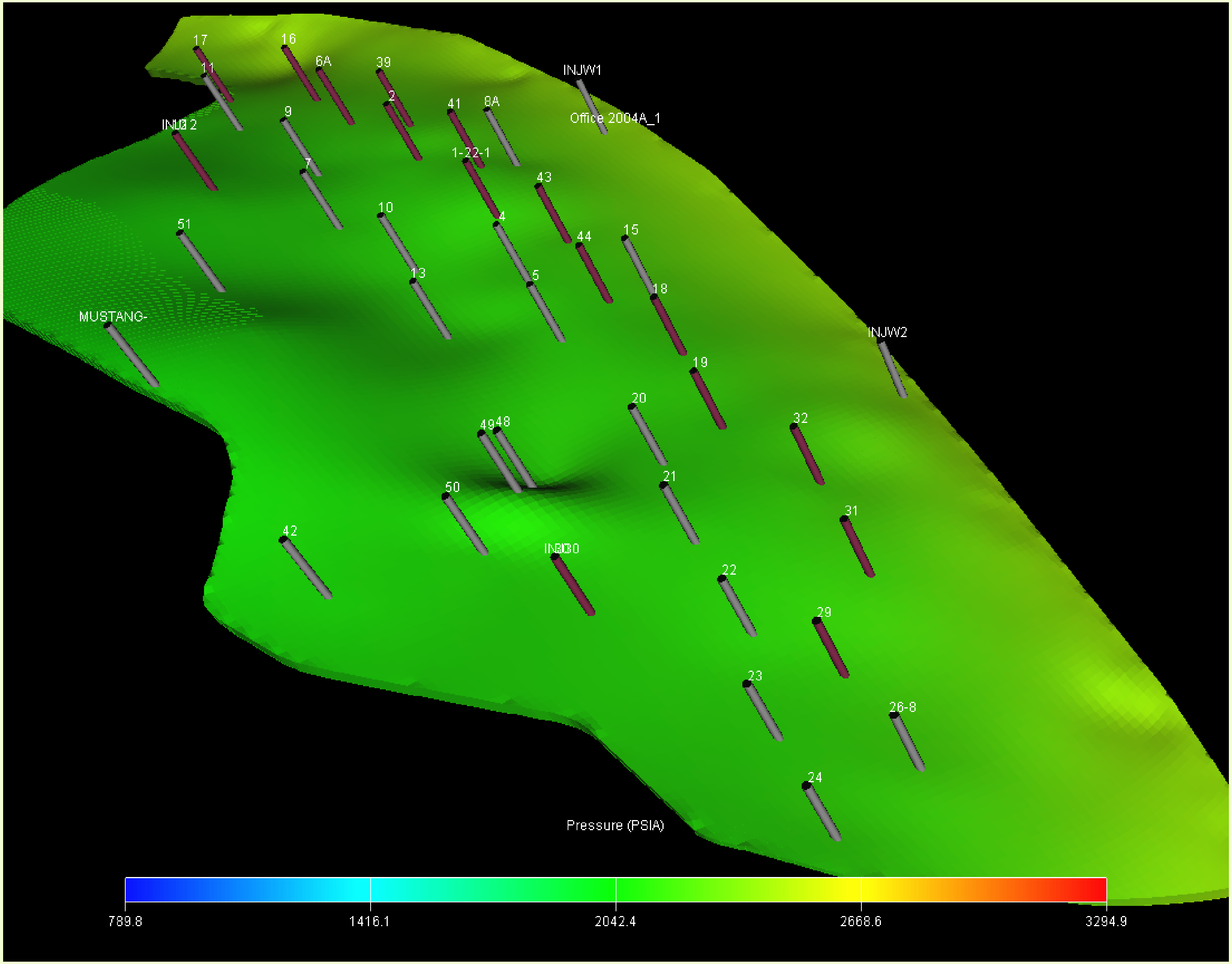

Figure 19. Simulated reservoir pressure distribution in August 1962.

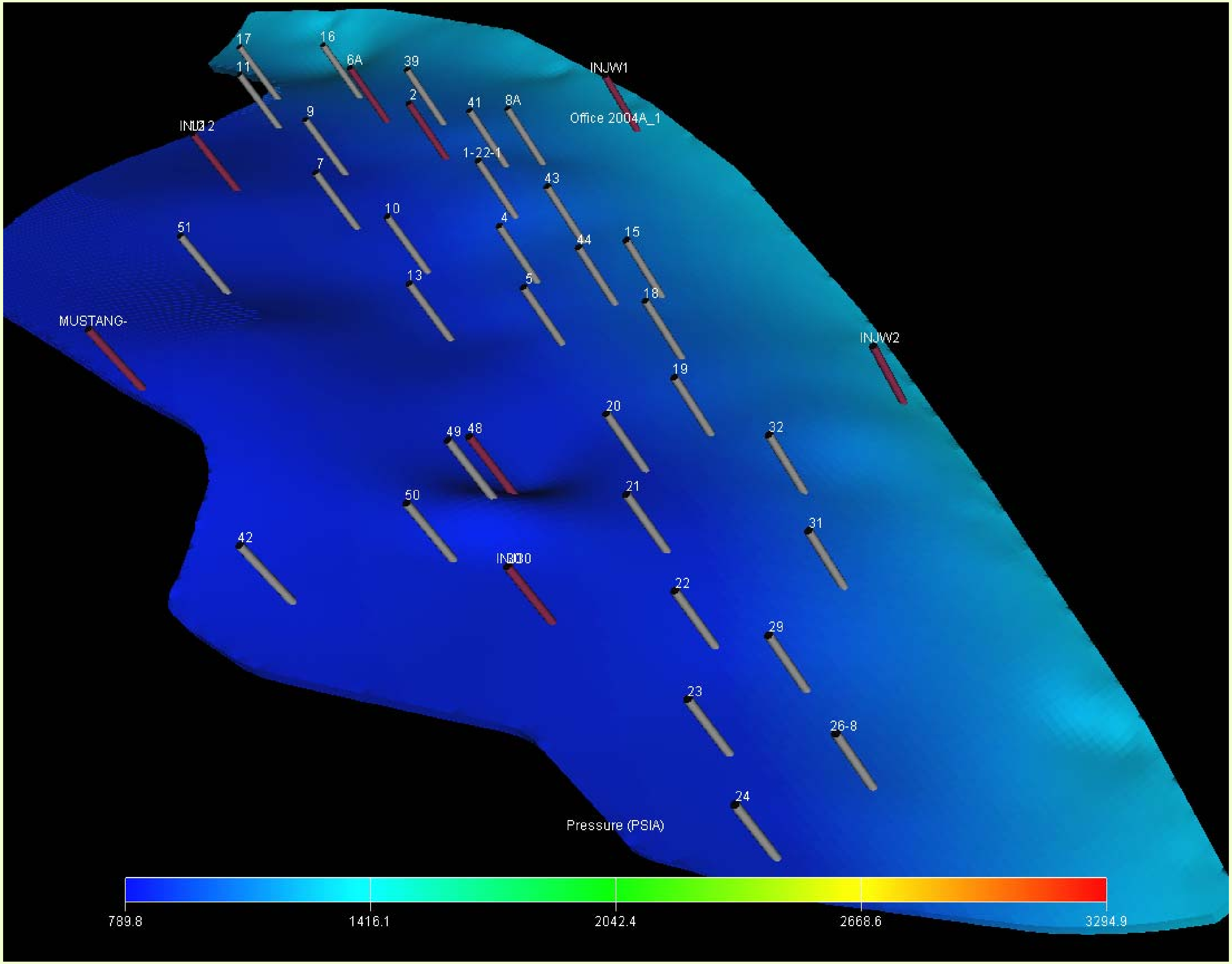

Figure 20. Simulated reservoir pressure distribution in March 1992.

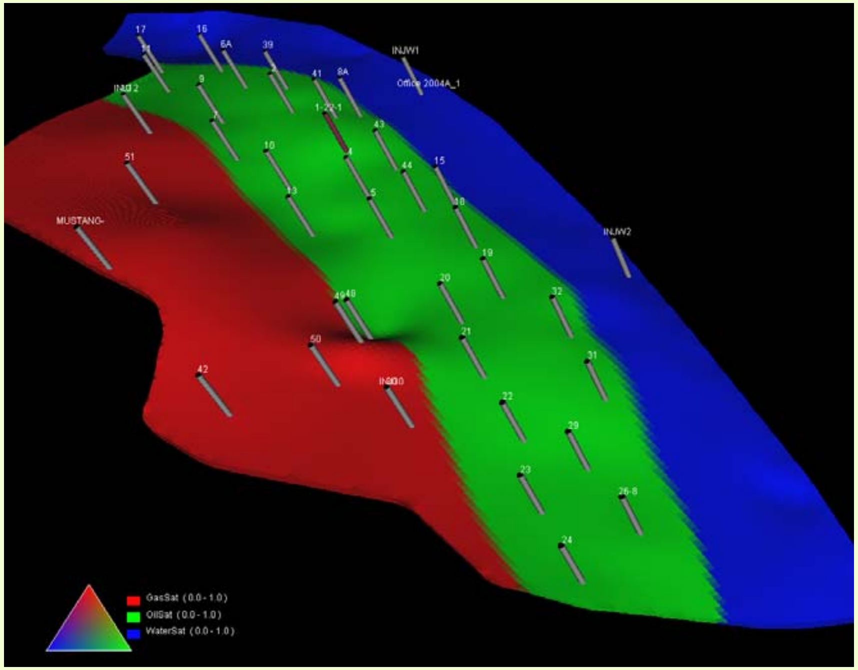

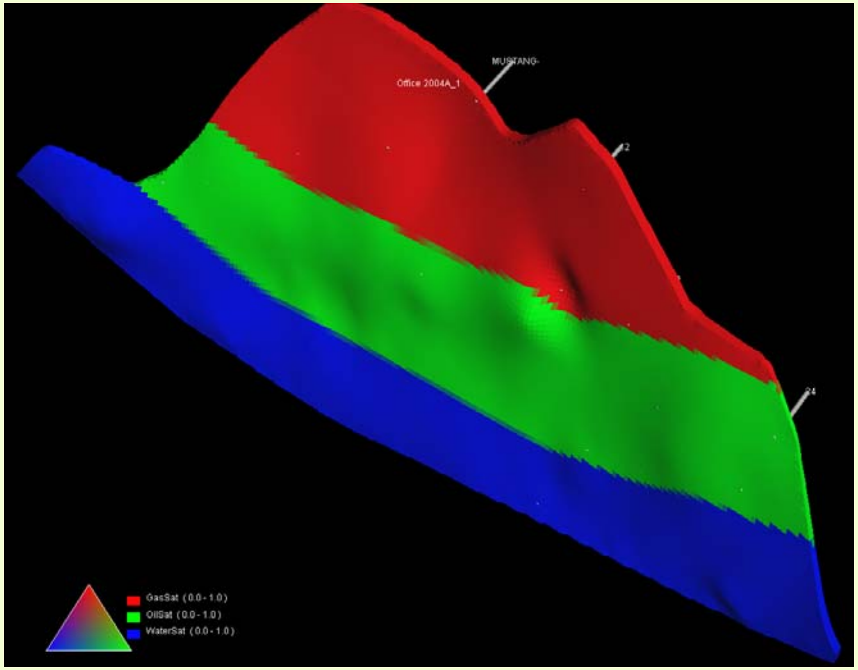

Figure 21. Initial oil, gas, and water distributions in August 1954, top view (left) and bottom view (right).

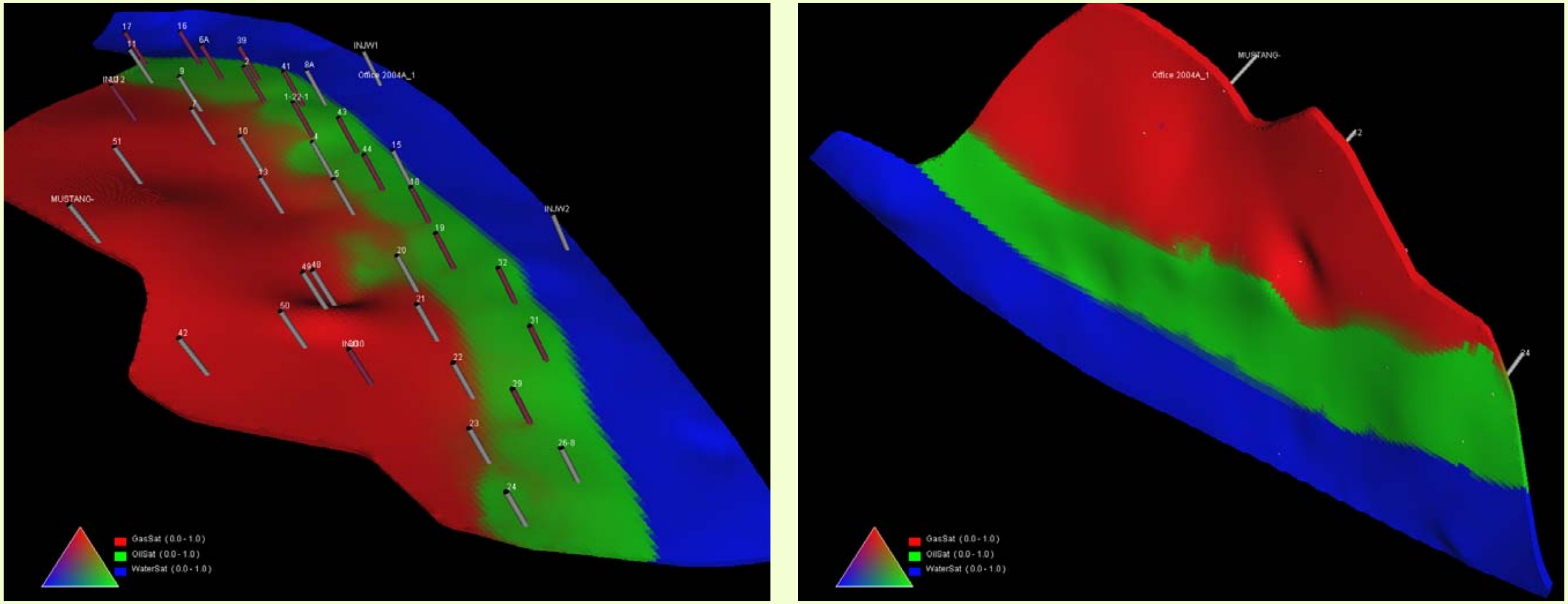

Figure 22. Ternary view of simulated oil, gas, and water distributions in August 1962, top view (left) and bottom view (right).

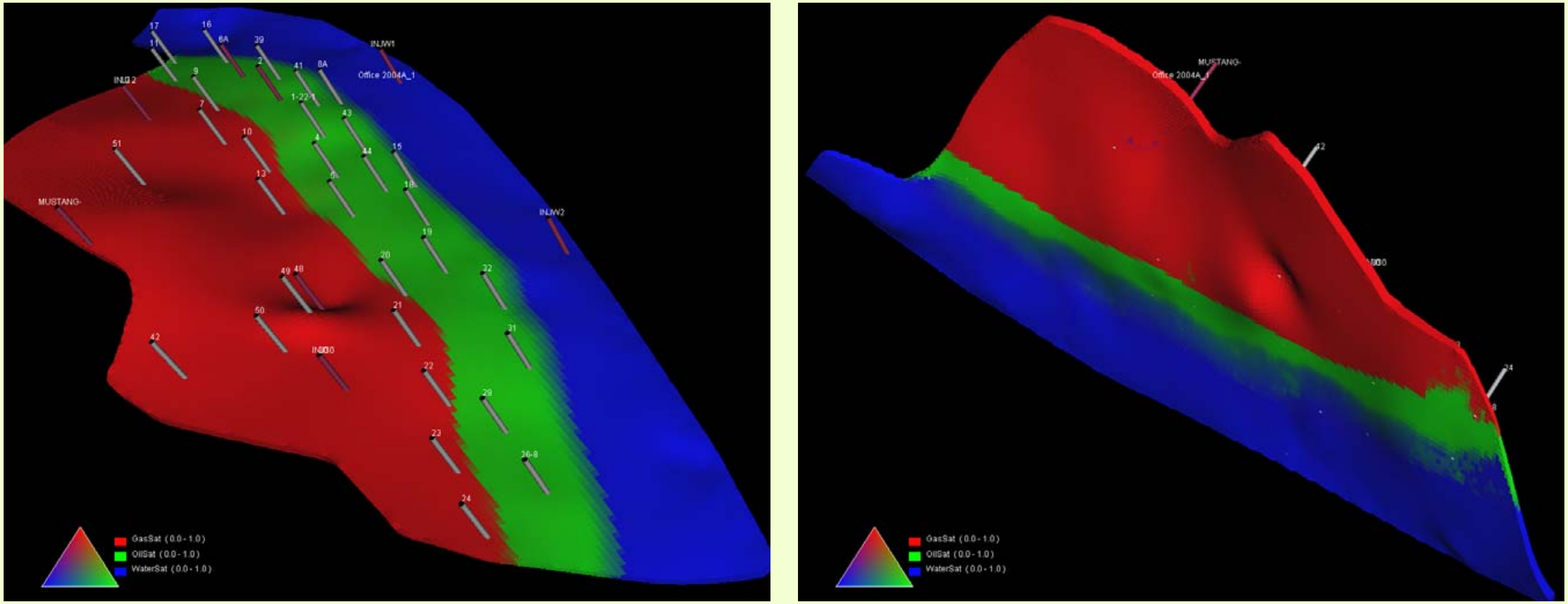

Figure 23. Ternary view of simulated oil, gas, and water distributions in March 1992, top view (left) and bottom view (right).

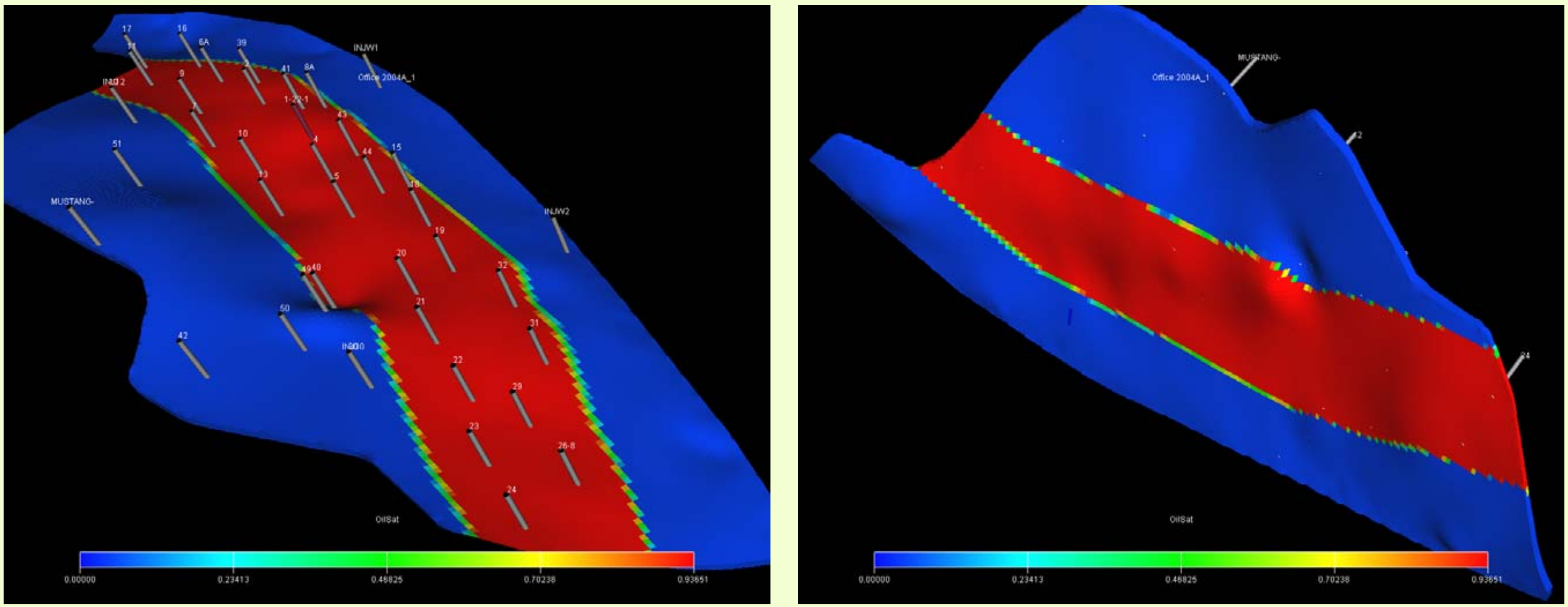

Figure 24. Initial reservoir oil saturation distribution in August 1954, top view (left) and bottom view (right).

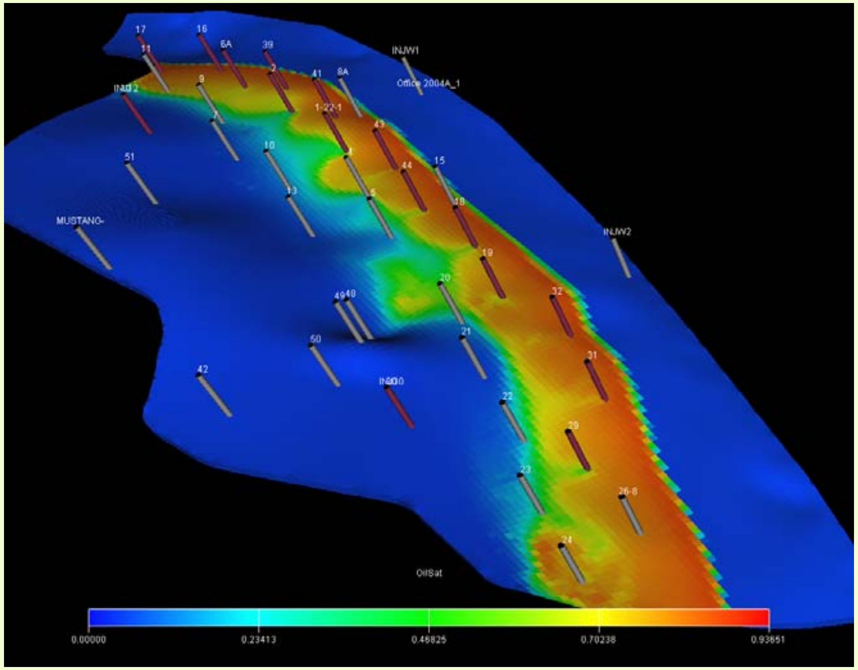

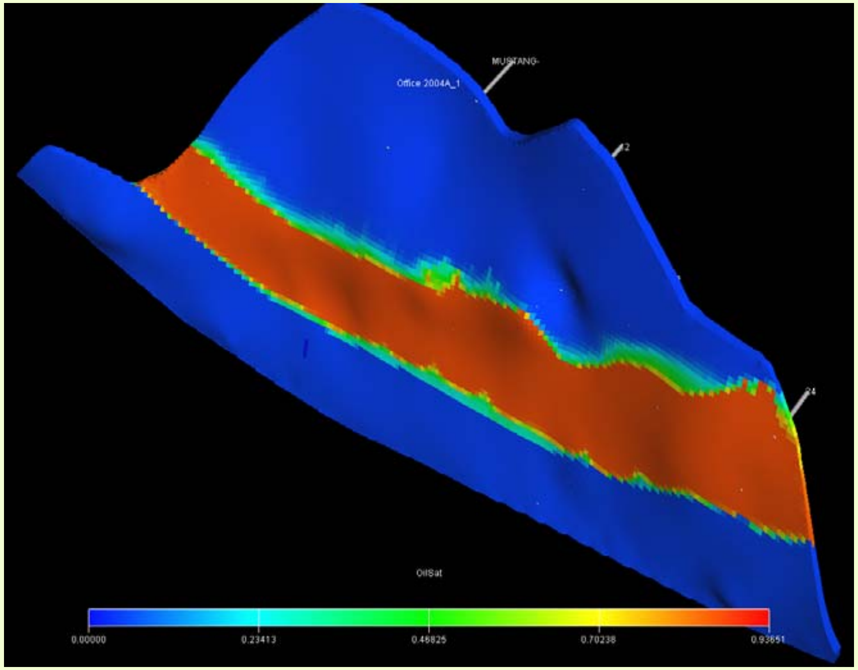

Figure 25. Simulated oil saturation distribution in August 1962, top view (left) and bottom view (right).

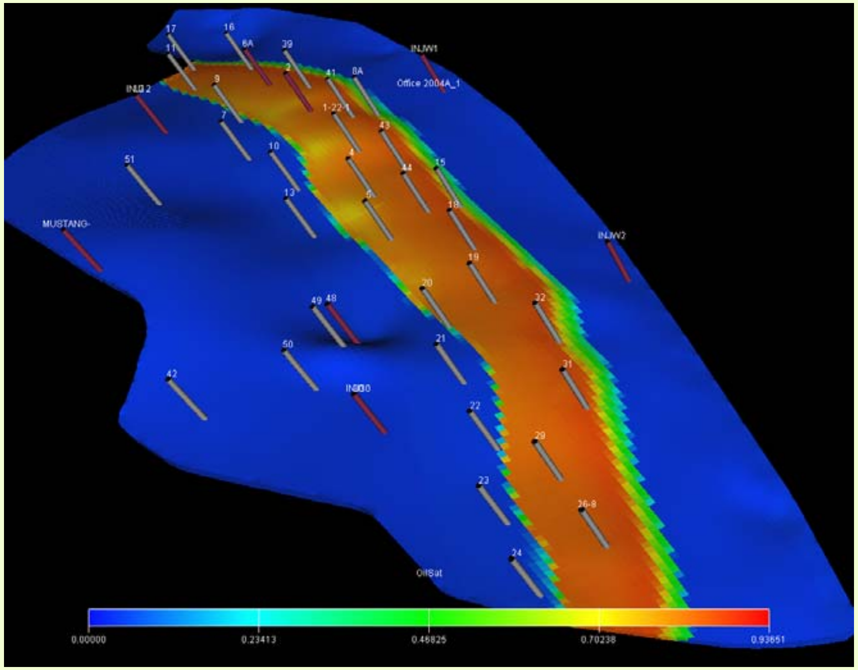

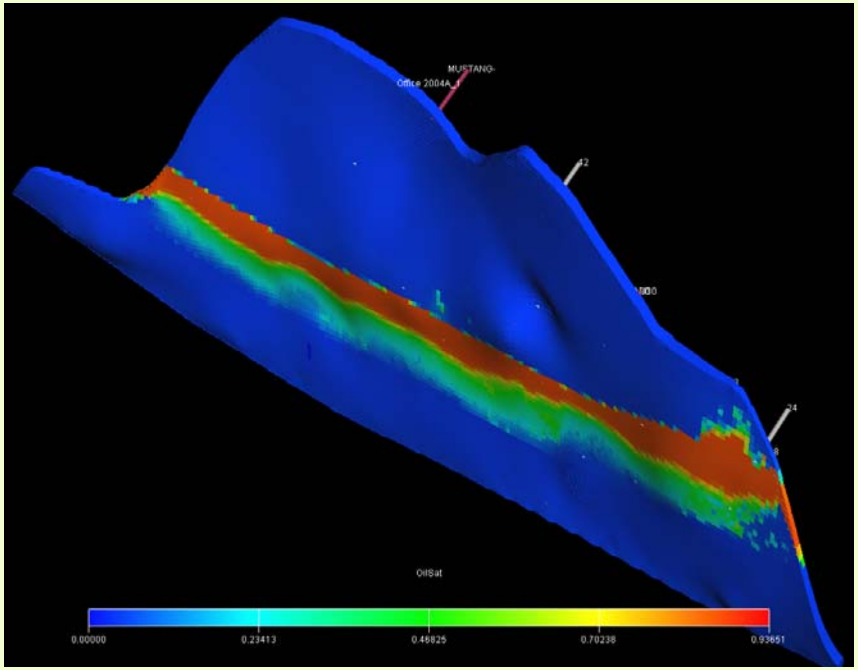

Figure 26. Simulated oil saturation distribution in March 1992, top view (left) and bottom view (right).

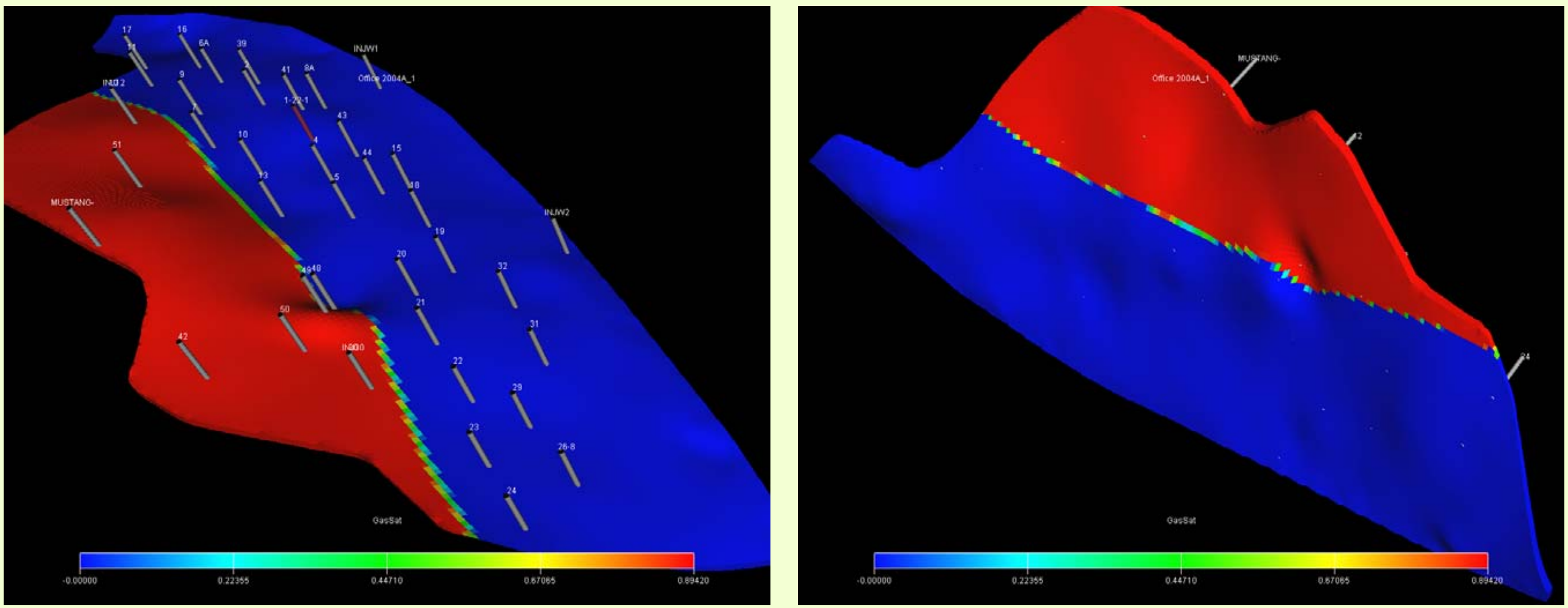

Figure 27. Initial reservoir gas saturation distribution in August 1954, top view (left) and bottom view (right).

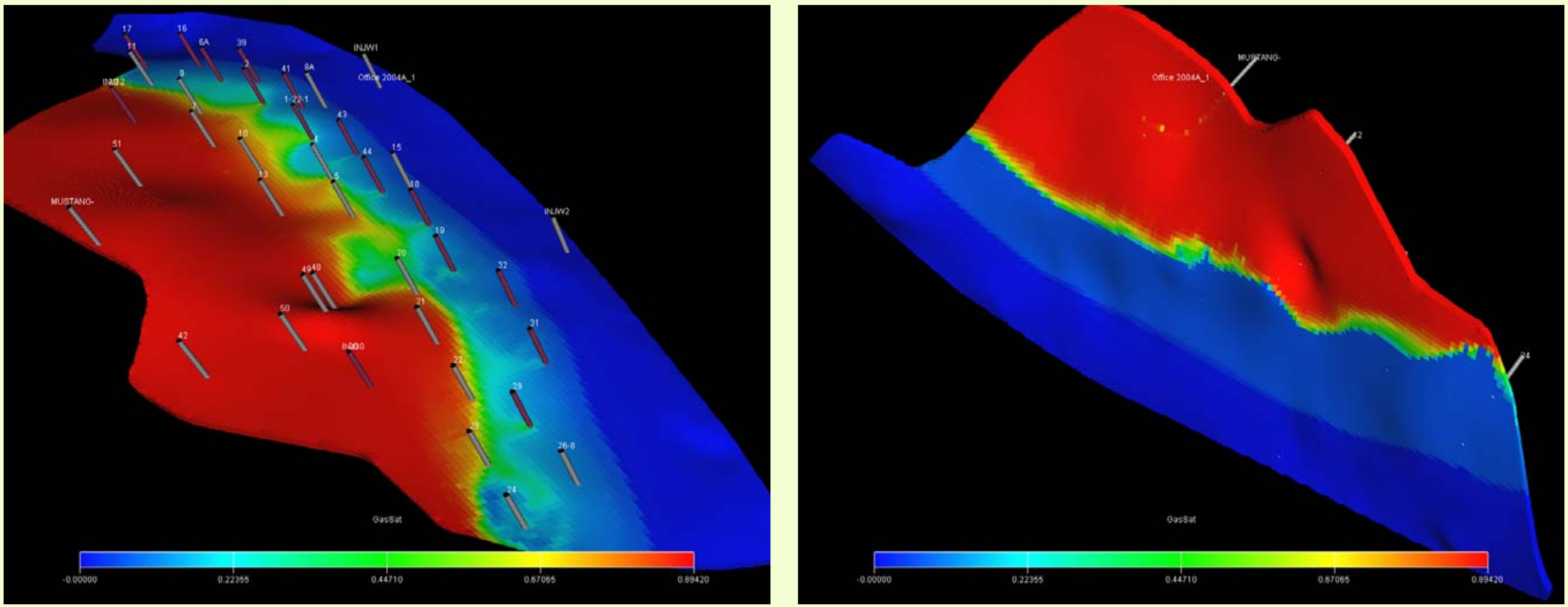

Figure 28. Simulated gas saturation distribution in August 1962, top view (left) and bottom view (right).

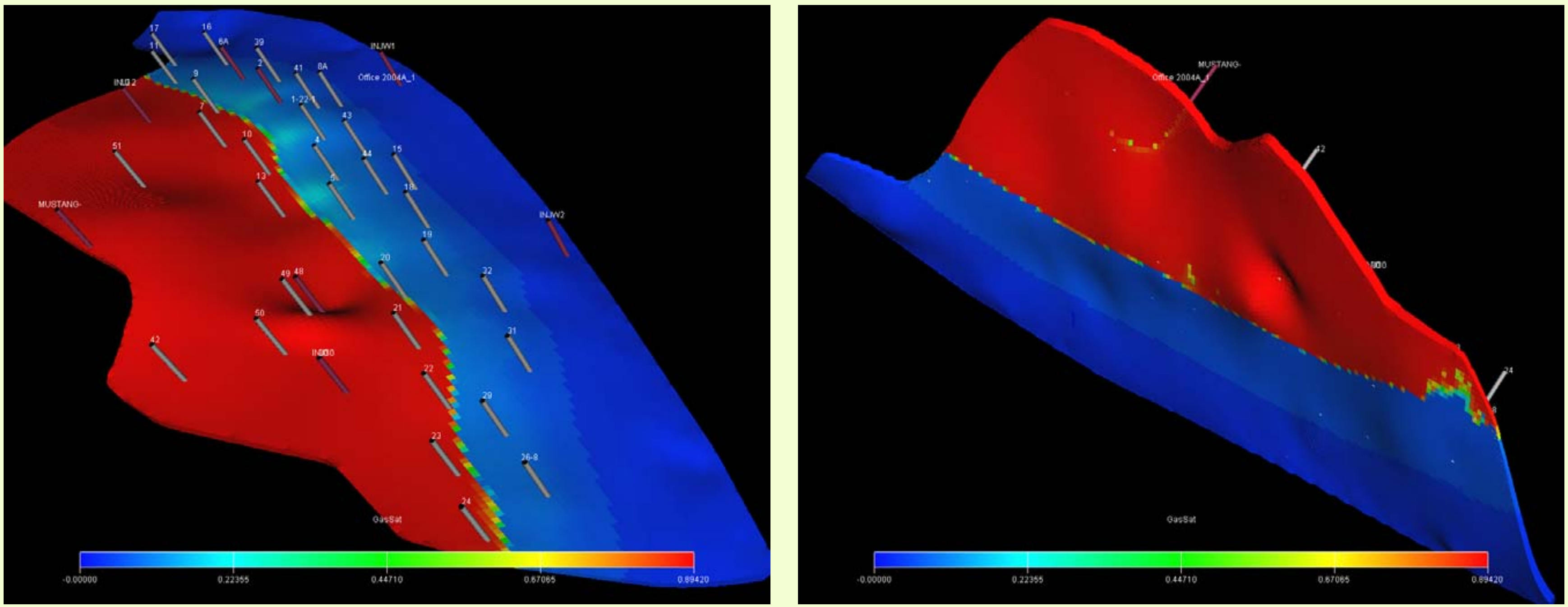

Figure 29. Simulated gas saturation distribution in March 1992, top view (left) and bottom view (right).

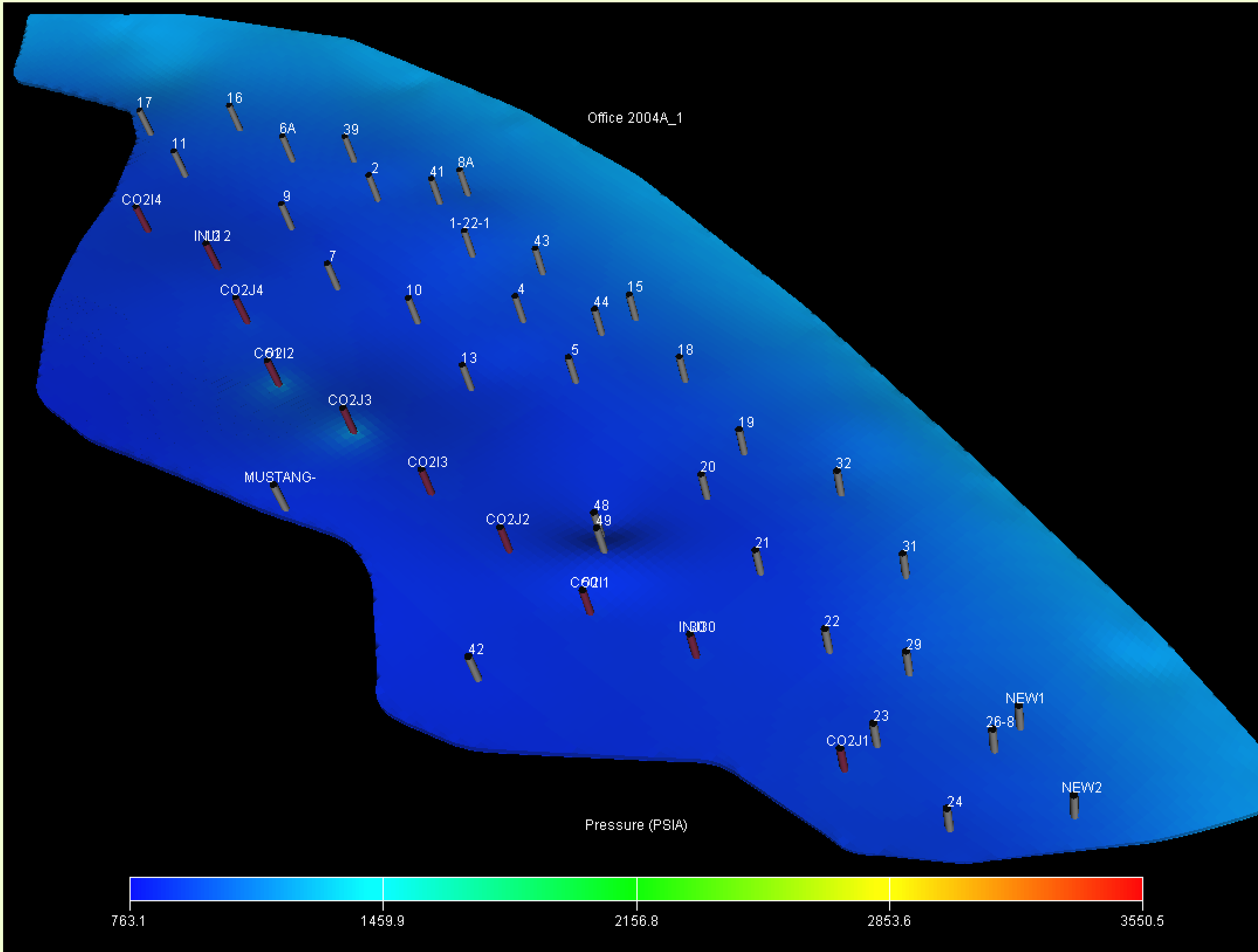

Figure 30. Reservoir pressure at the beginning of CO2 injection and injection/production well locations.

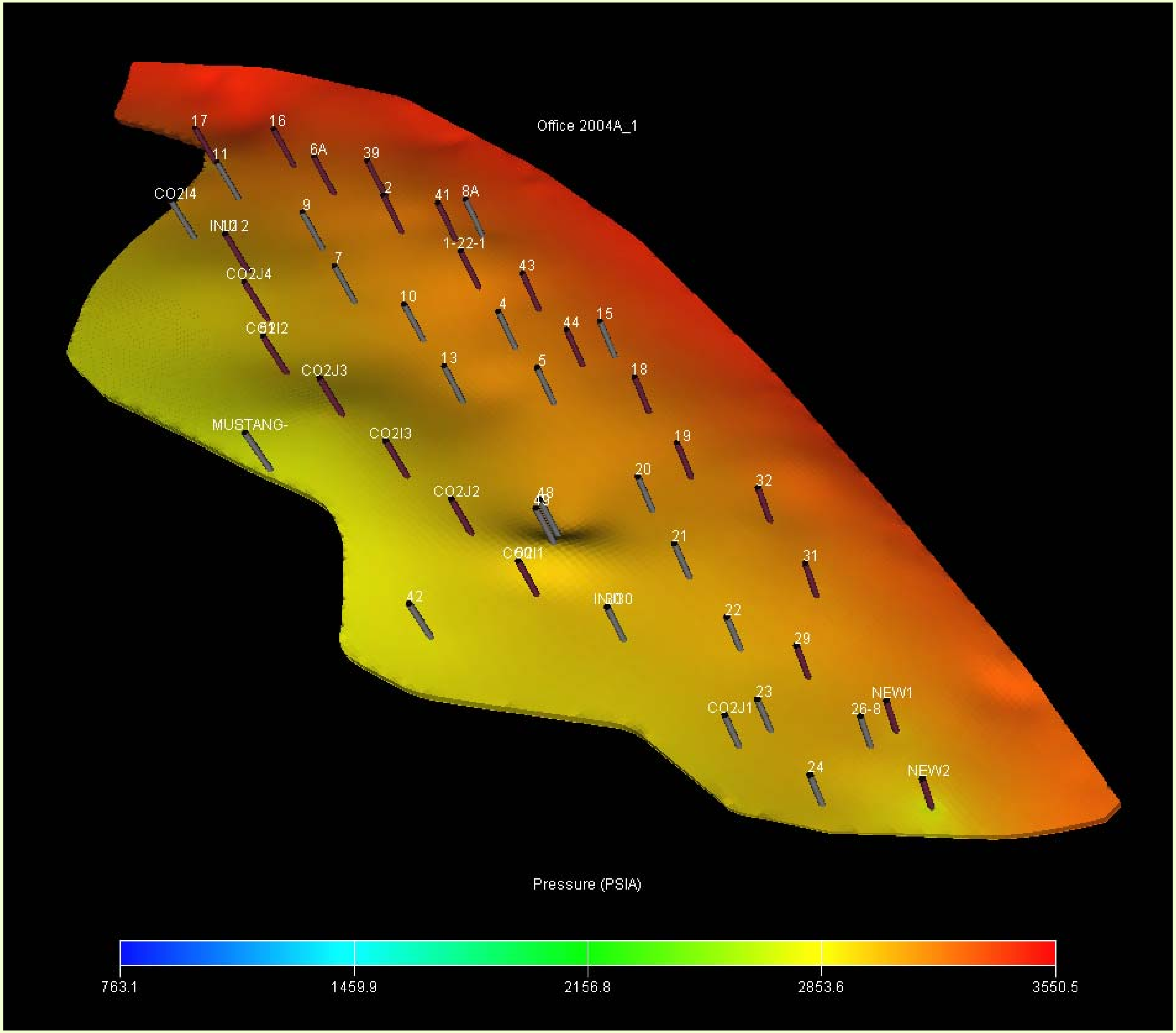

Figure 31. Reservoir pressure at the beginning of the production phase in Scenario 3.

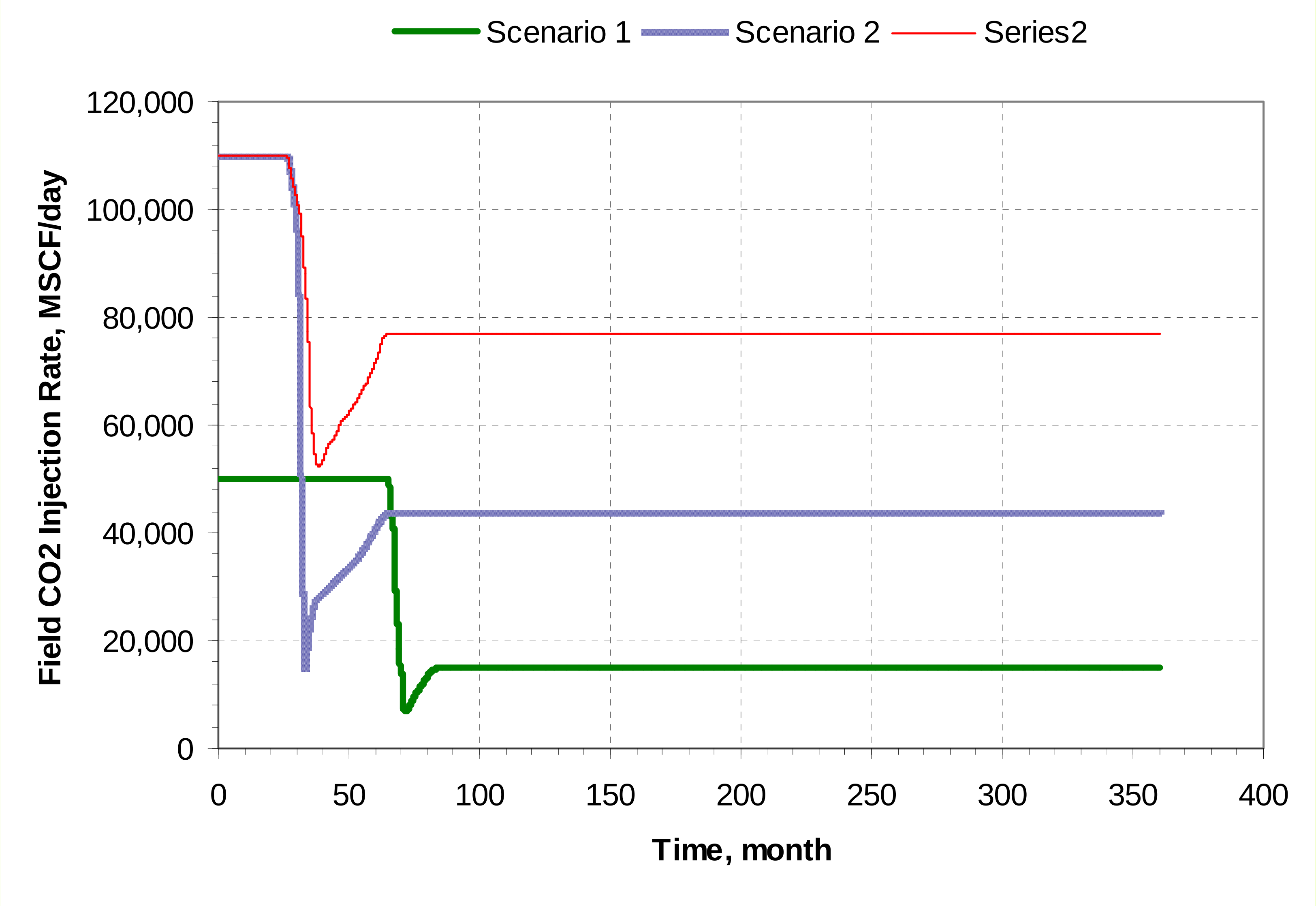

Figure 32. Field CO2 injection rates of the three simulated scenarios.

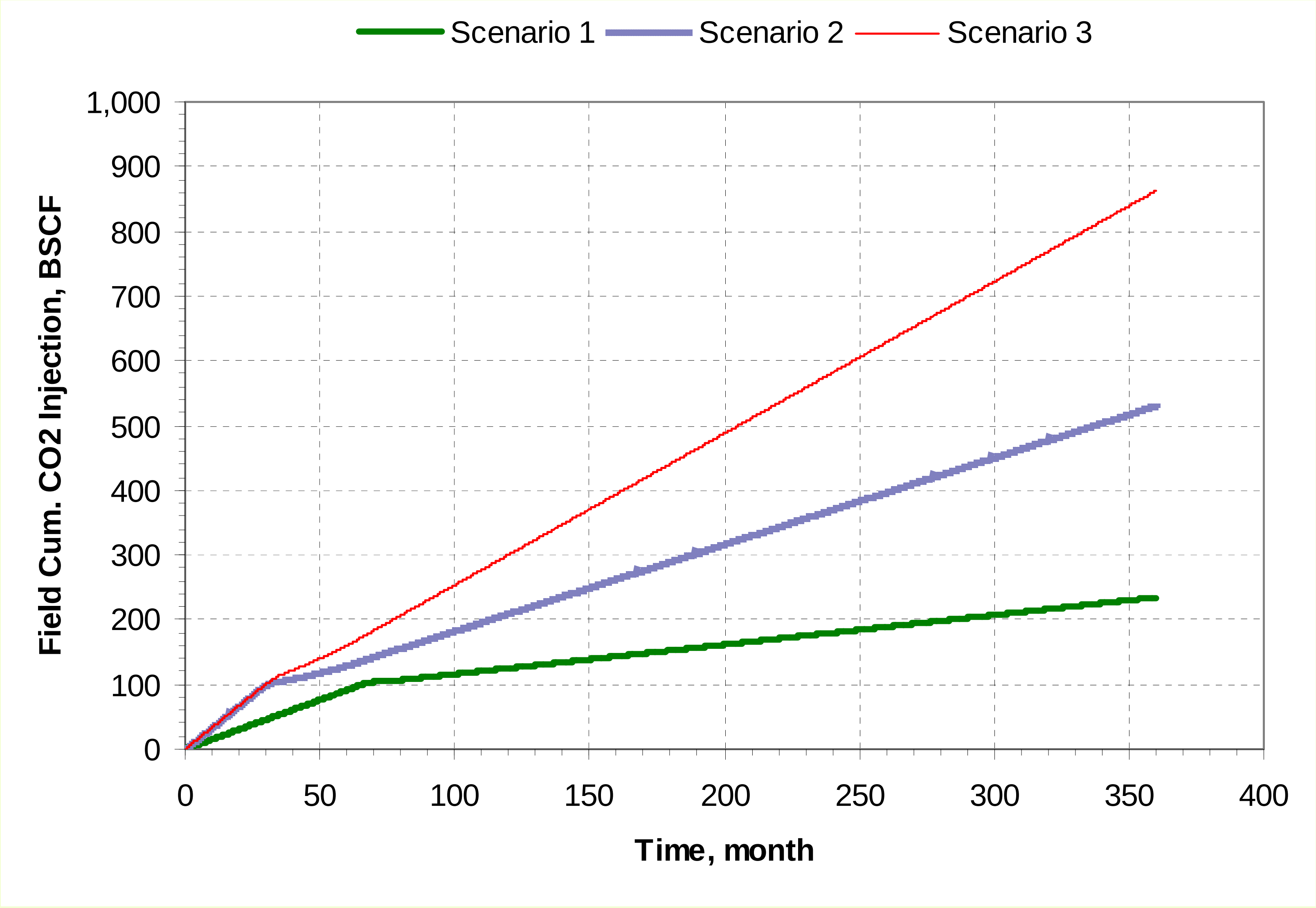

Figure 33. Field cumulative CO2 injection volumes of the three simulated scenarios.

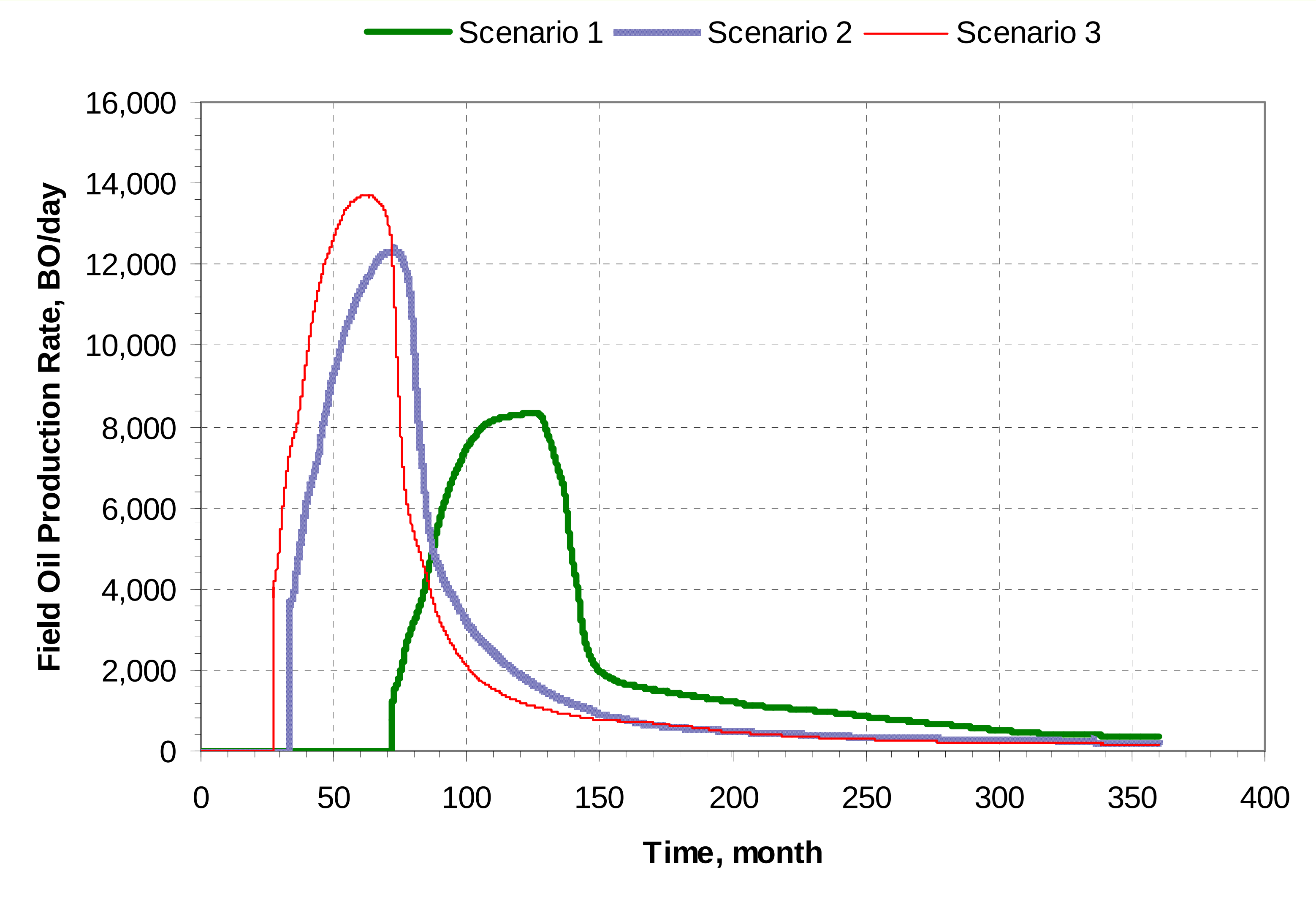

Figure 34. Field oil production rates of the three simulated scenarios.

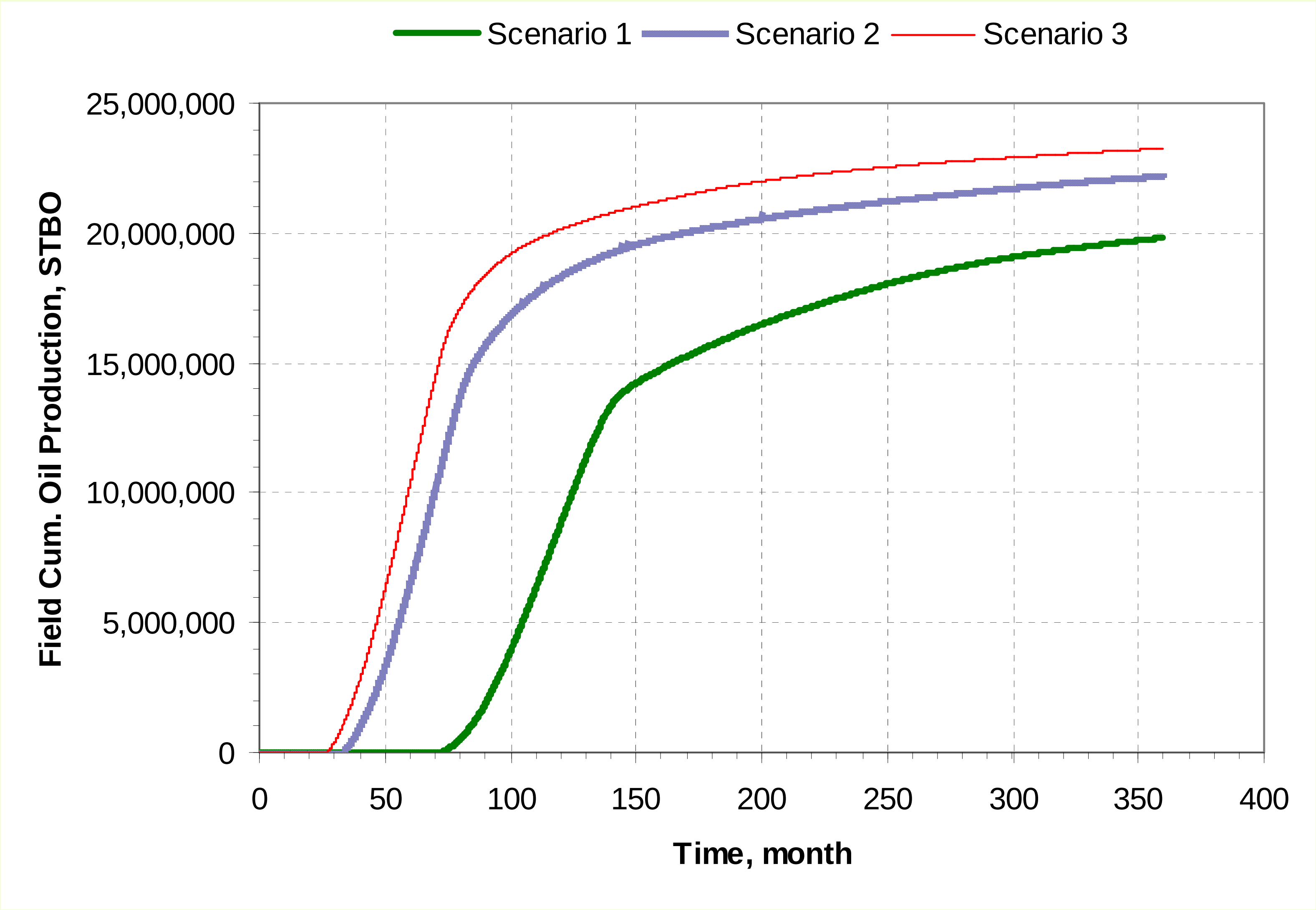

Figure 35. Field cumulative oil productions of the three simulated scenarios.

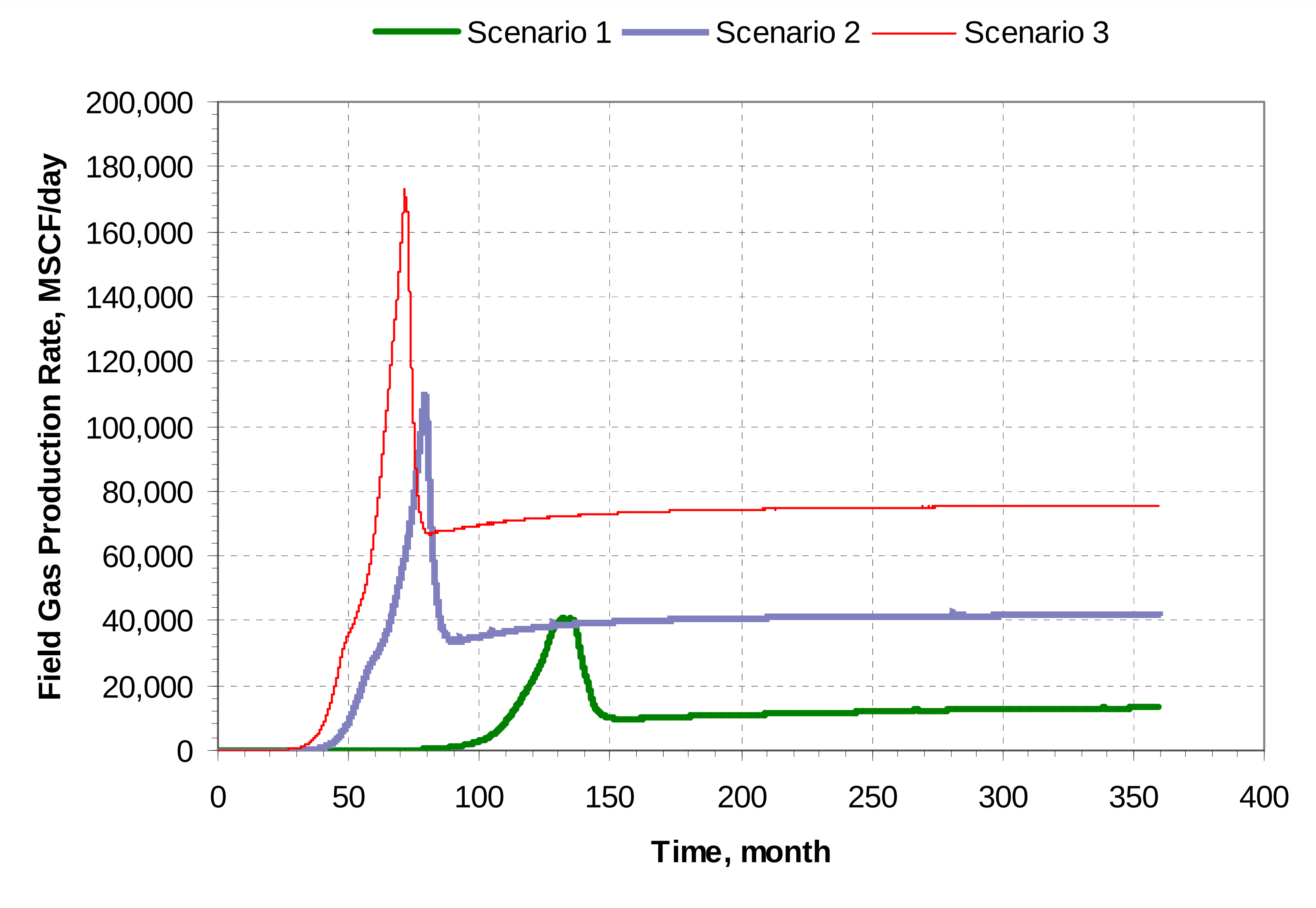

Figure 36. Field gas production rates of the three simulated scenarios.

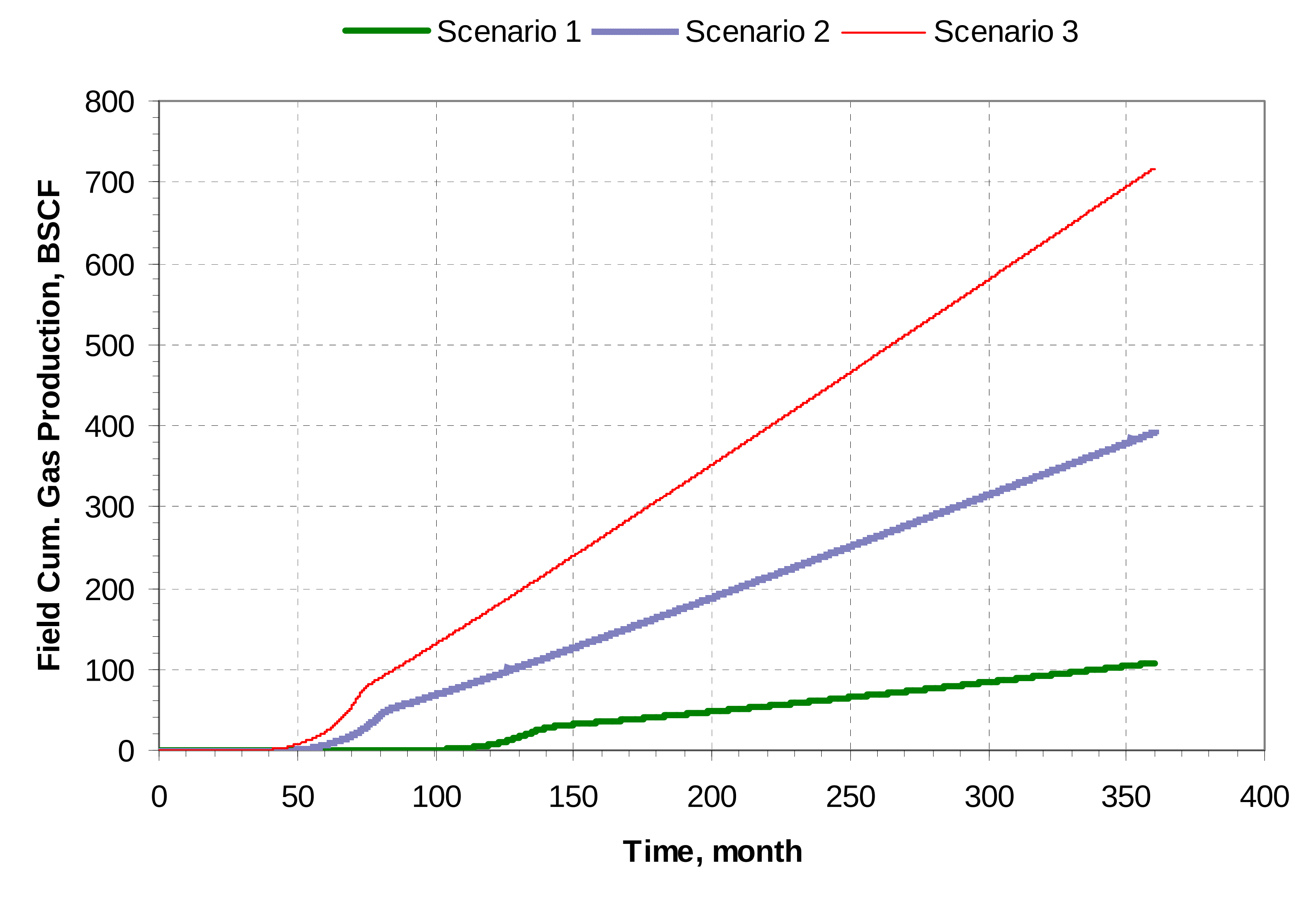

Figure 37. Field cumulative gas productions of the three simulated scenarios.

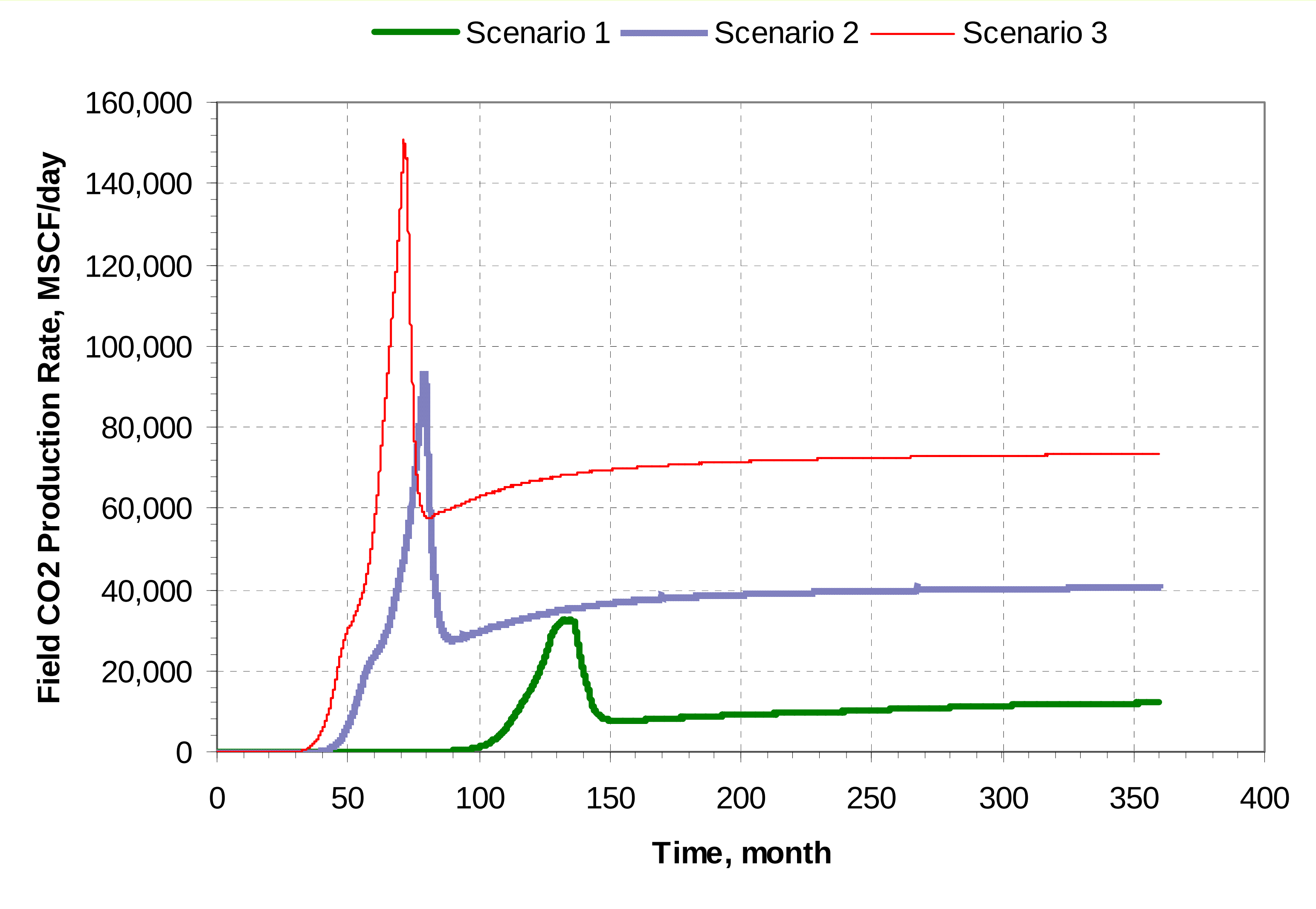

Figure 38. Field CO2 production rates of the three simulated scenarios.

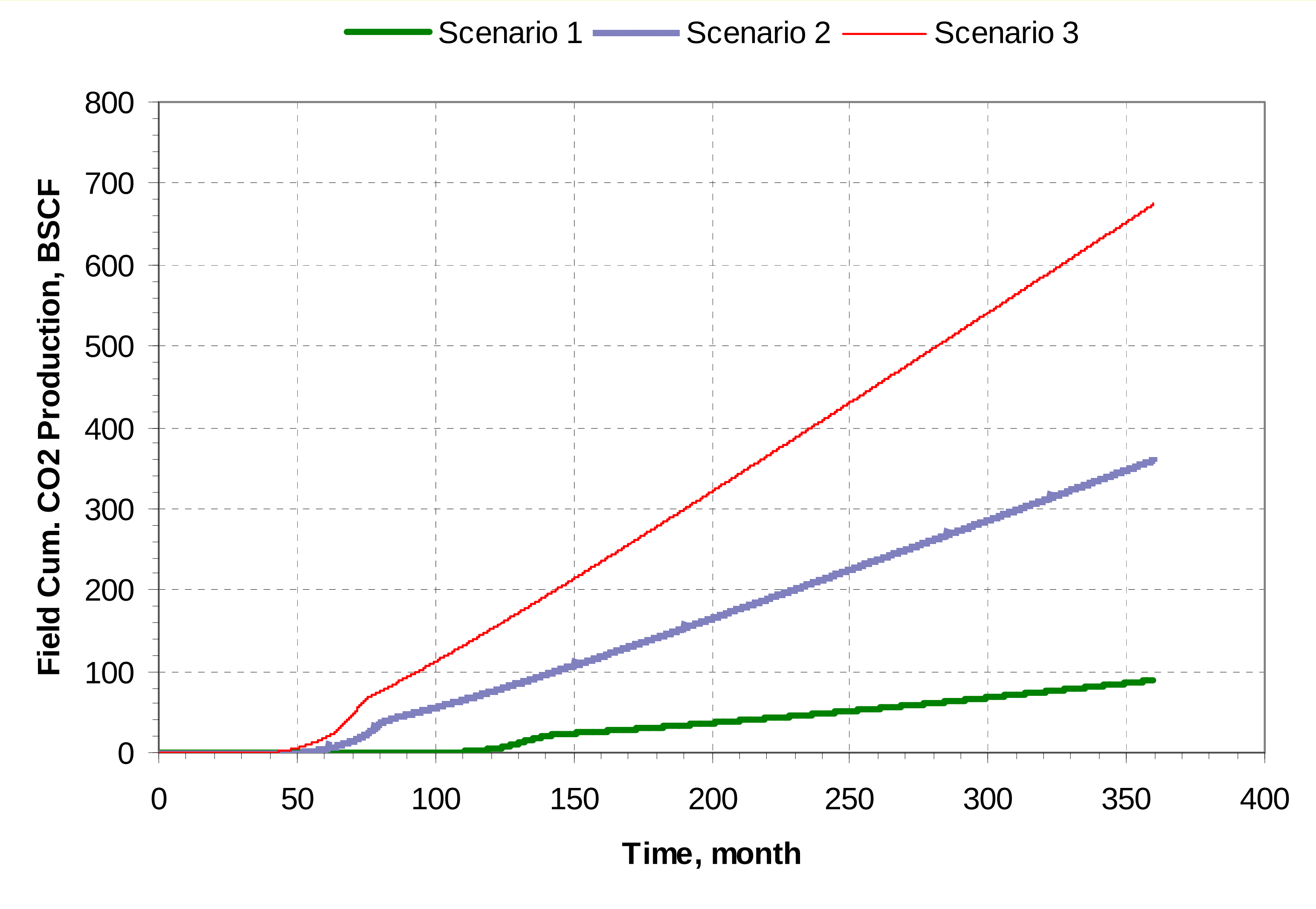

Figure 39. Field cumulative CO2 productions of the three simulated scenarios.

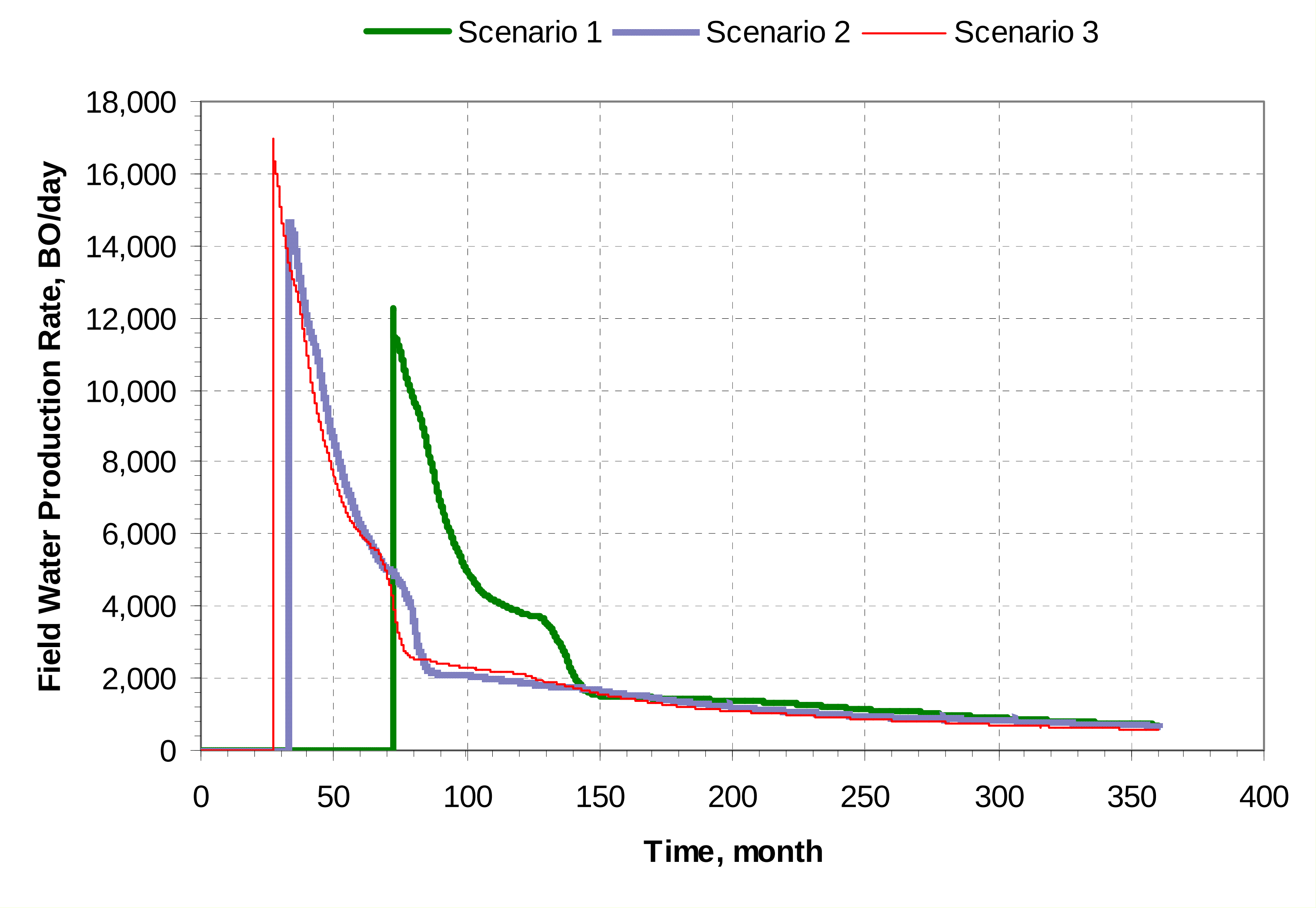

Figure 40. Field water production rates of the three simulated scenarios.

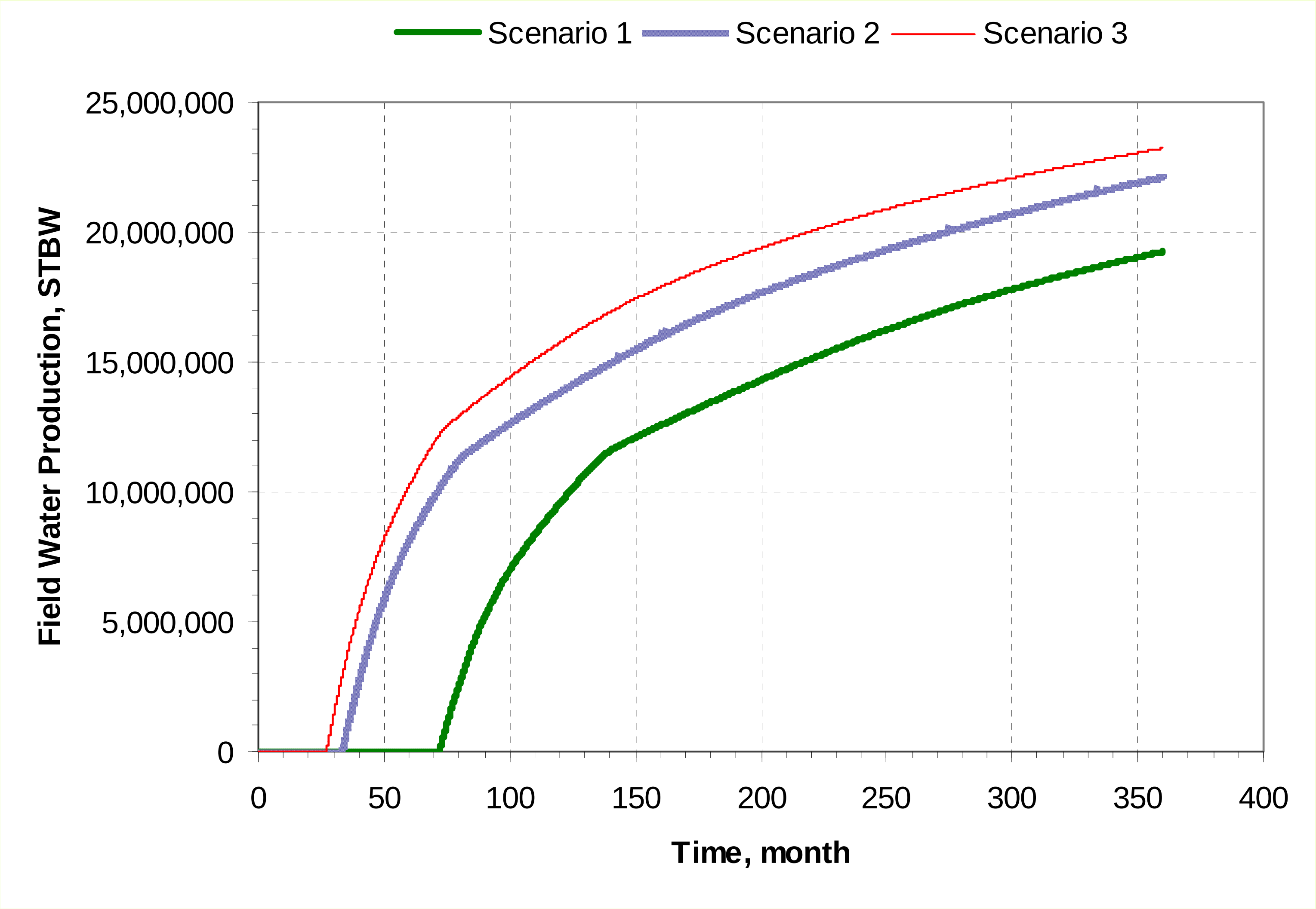

Figure 41. Field cumulative water productions of the three simulated scenarios.

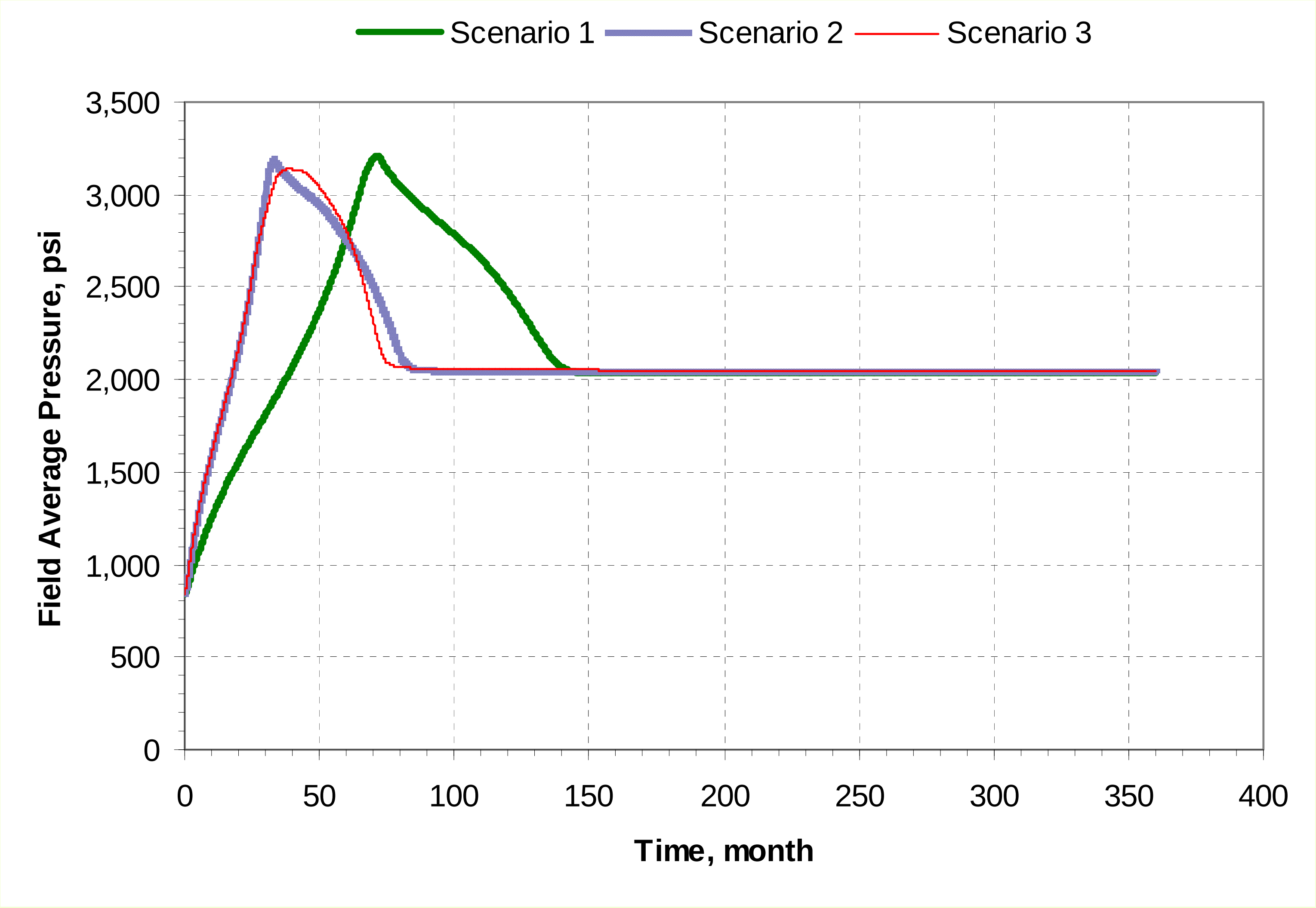

Figure 42. Field average pressure during both repressurization and production phases.

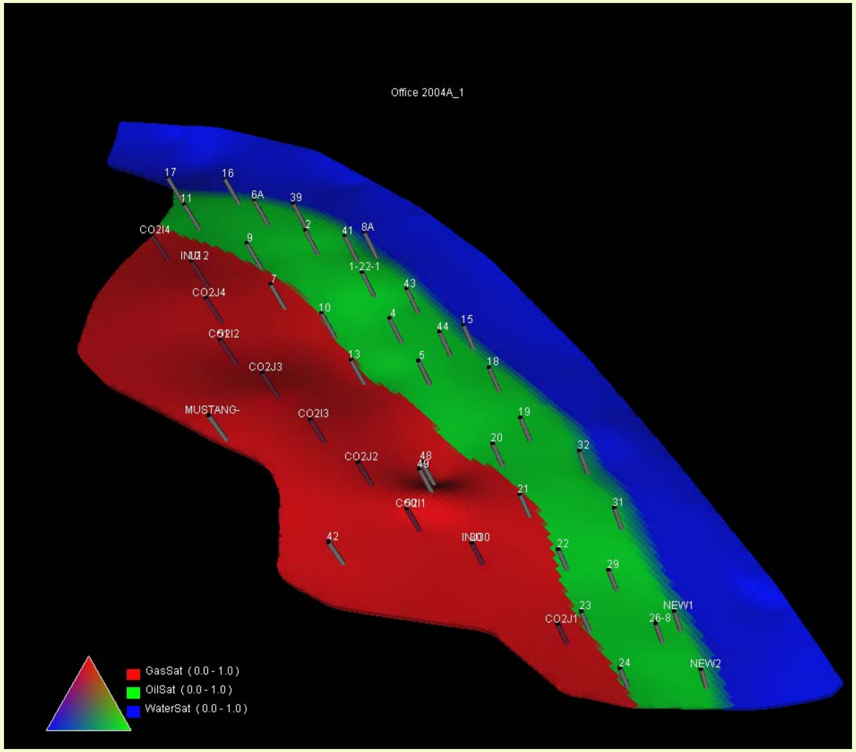

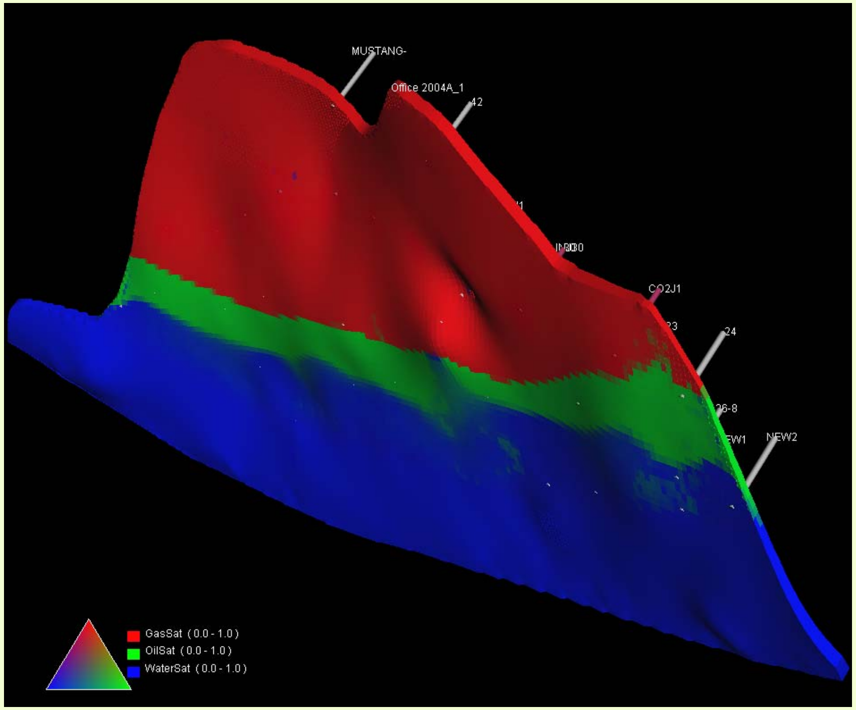

Figure 43. Ternary view of oil, gas, and water distributions at the beginning of CO2 injection in Scenario 3, top view (left) and bottom view (right).

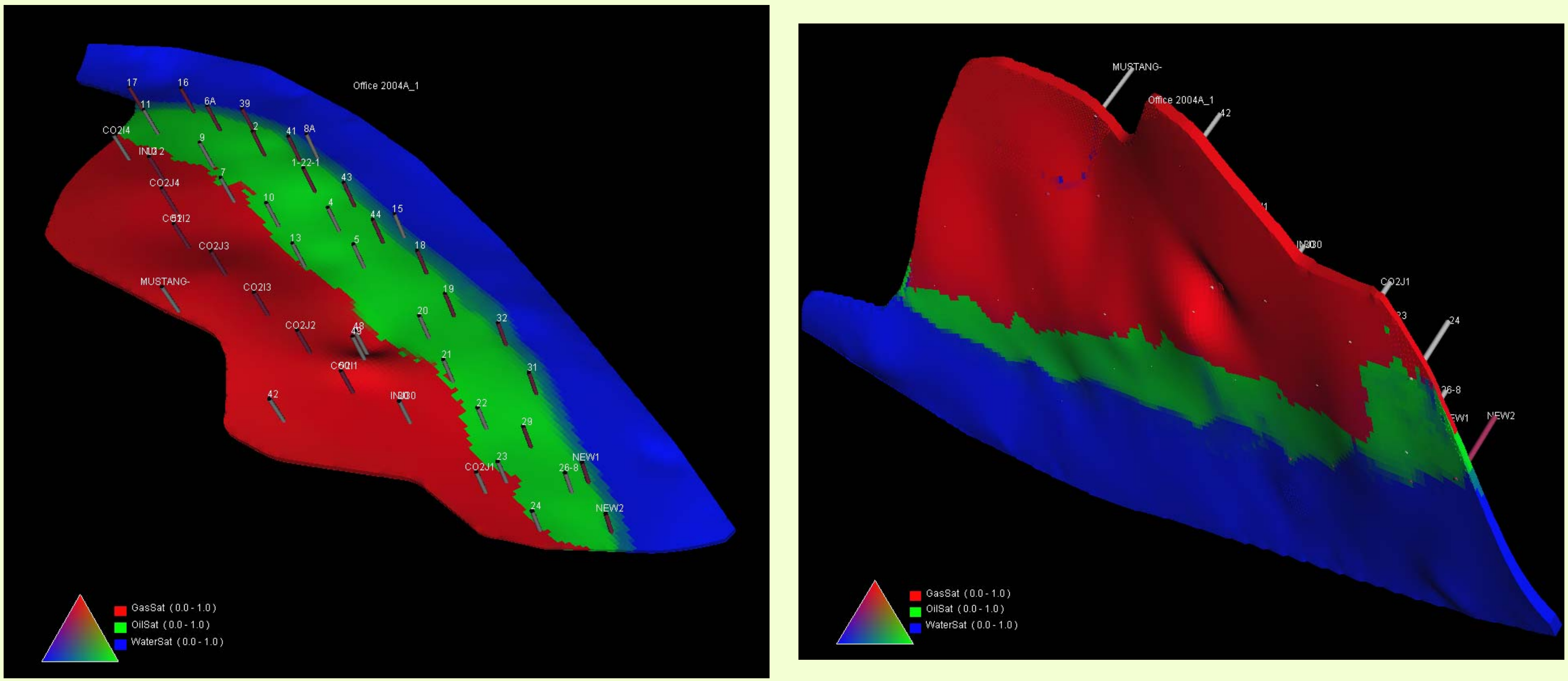

Figure 44. Ternary view of oil, gas, and water distributions after 27 months of CO2 injection followed by 21-month injection/production in Scenario 3, top view (left) and bottom view (right).

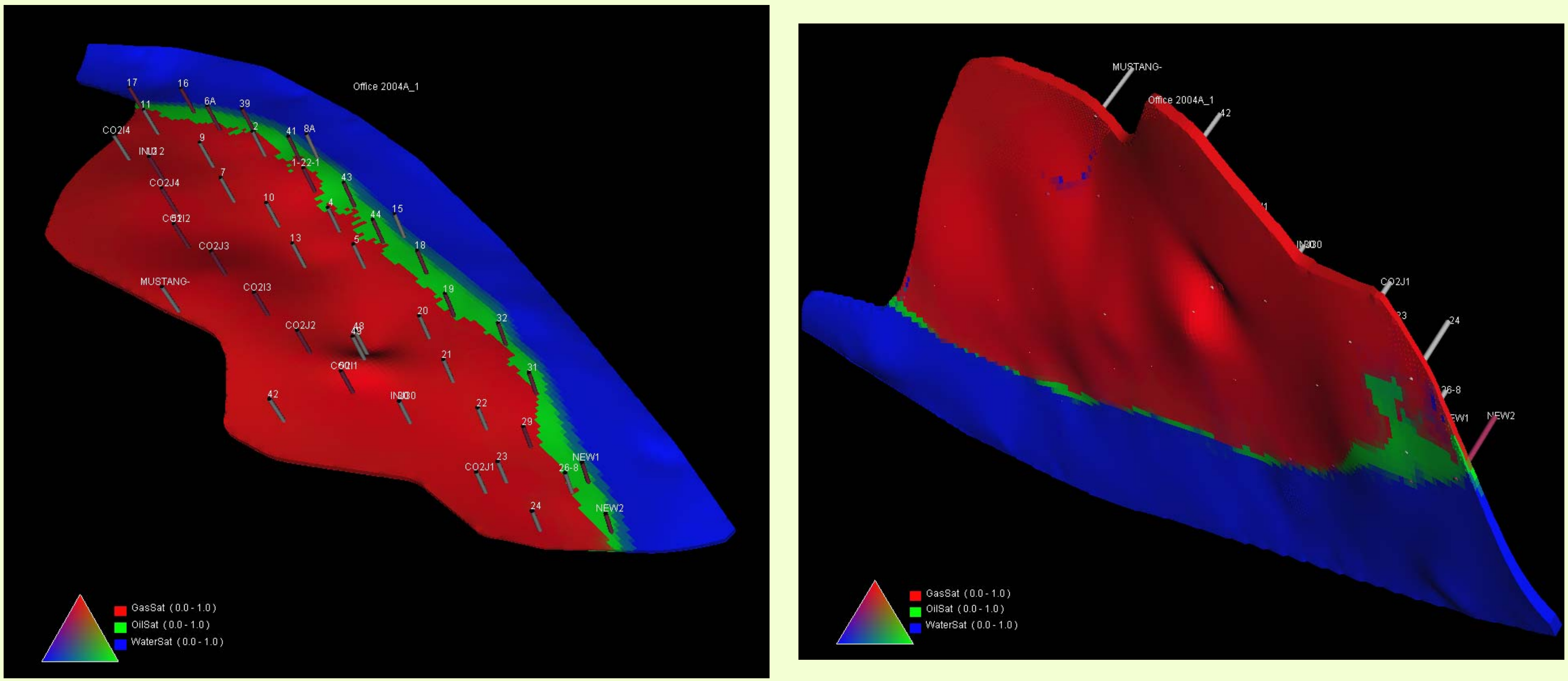

Figure 45. Ternary view of oil, gas, and water distributions at the end of a 14-year CO2 flooding operation in Scenario 3, top view (left) and bottom view (right).

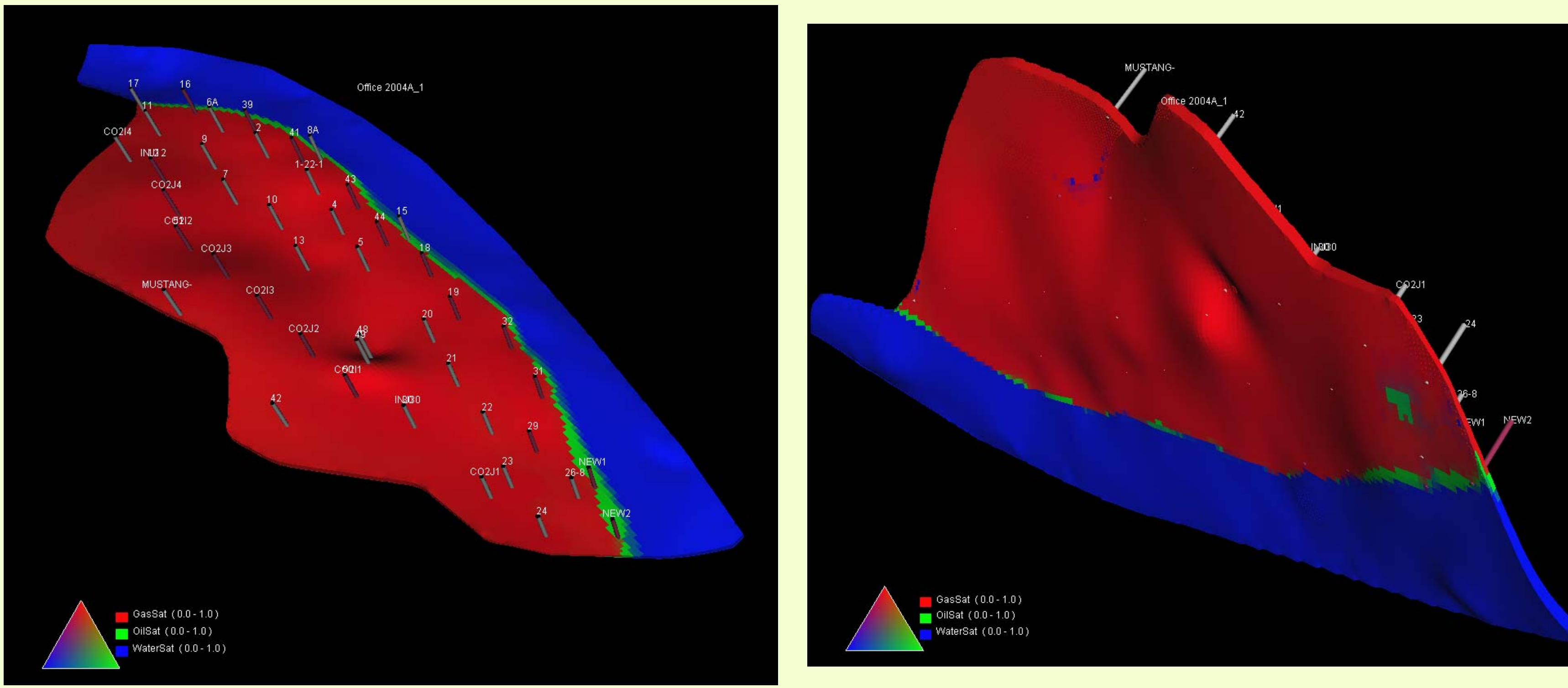

Figure 46. Ternary view of oil, gas, and water distributions at the end of a 30-year CO2 flooding operation in Scenario 3, top view (left) and bottom view (right).

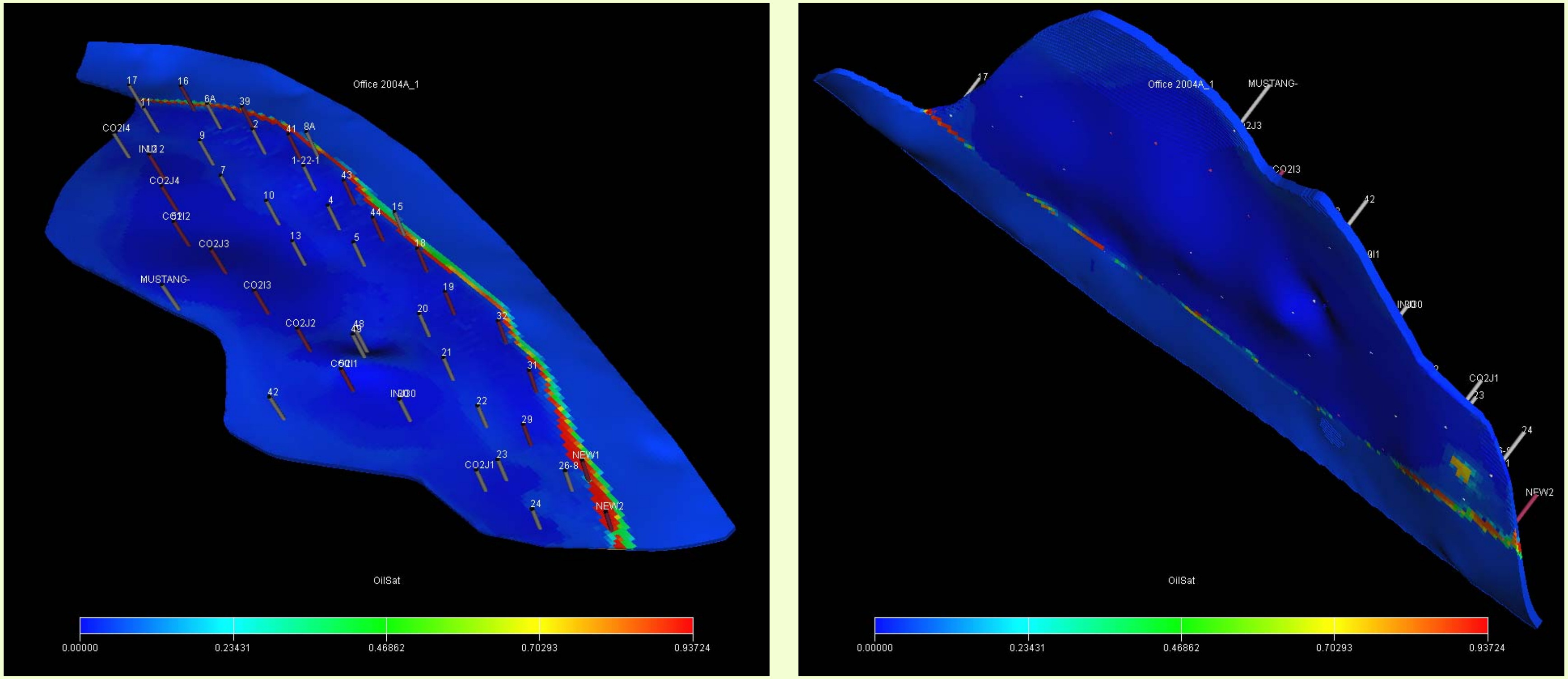

Figure 47. Reservoir oil saturation at the end of a 30-year CO2 flooding in Scenario 3, top view (left) and bottom view (right).

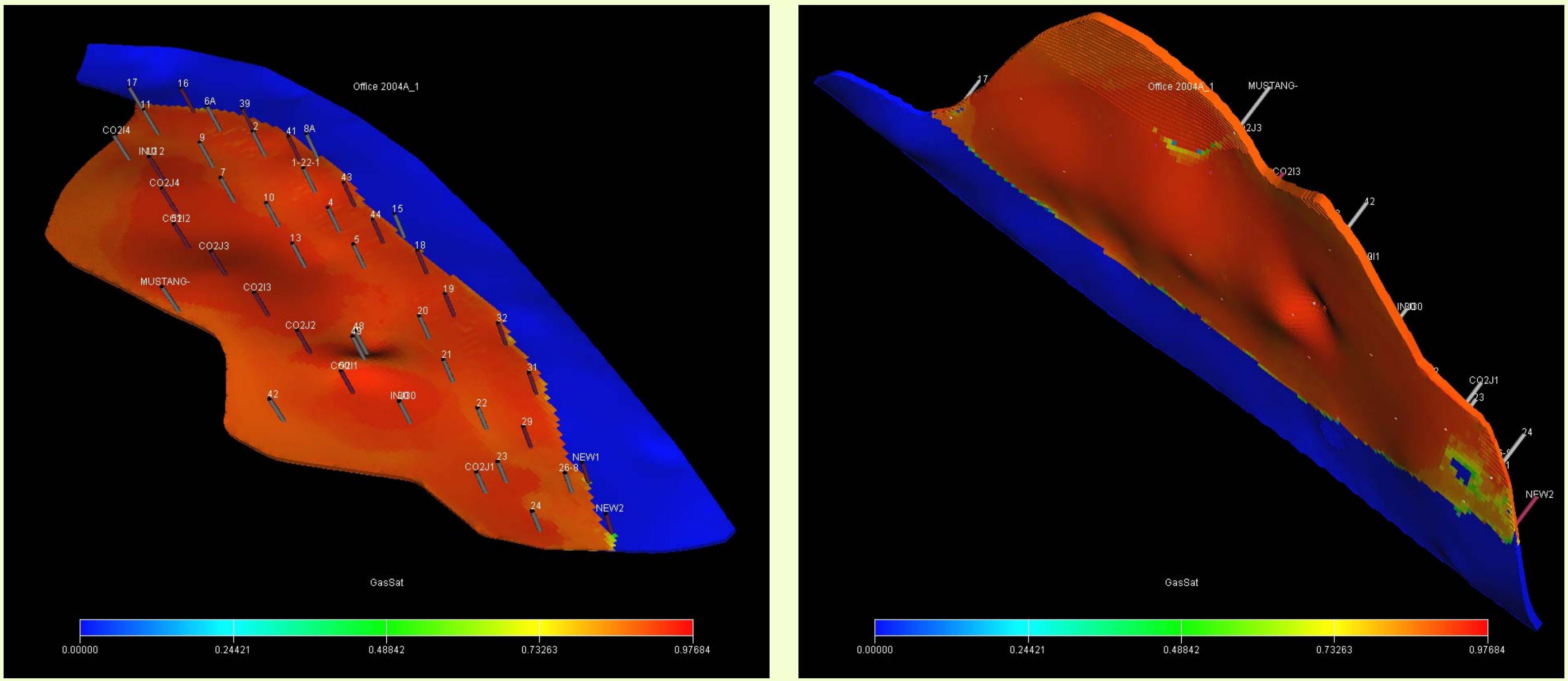

Figure 48. Reservoir gas saturation (including CO2) at the end of a 30-year CO2 flooding in Scenario 3, top view (left) and bottom view (right).

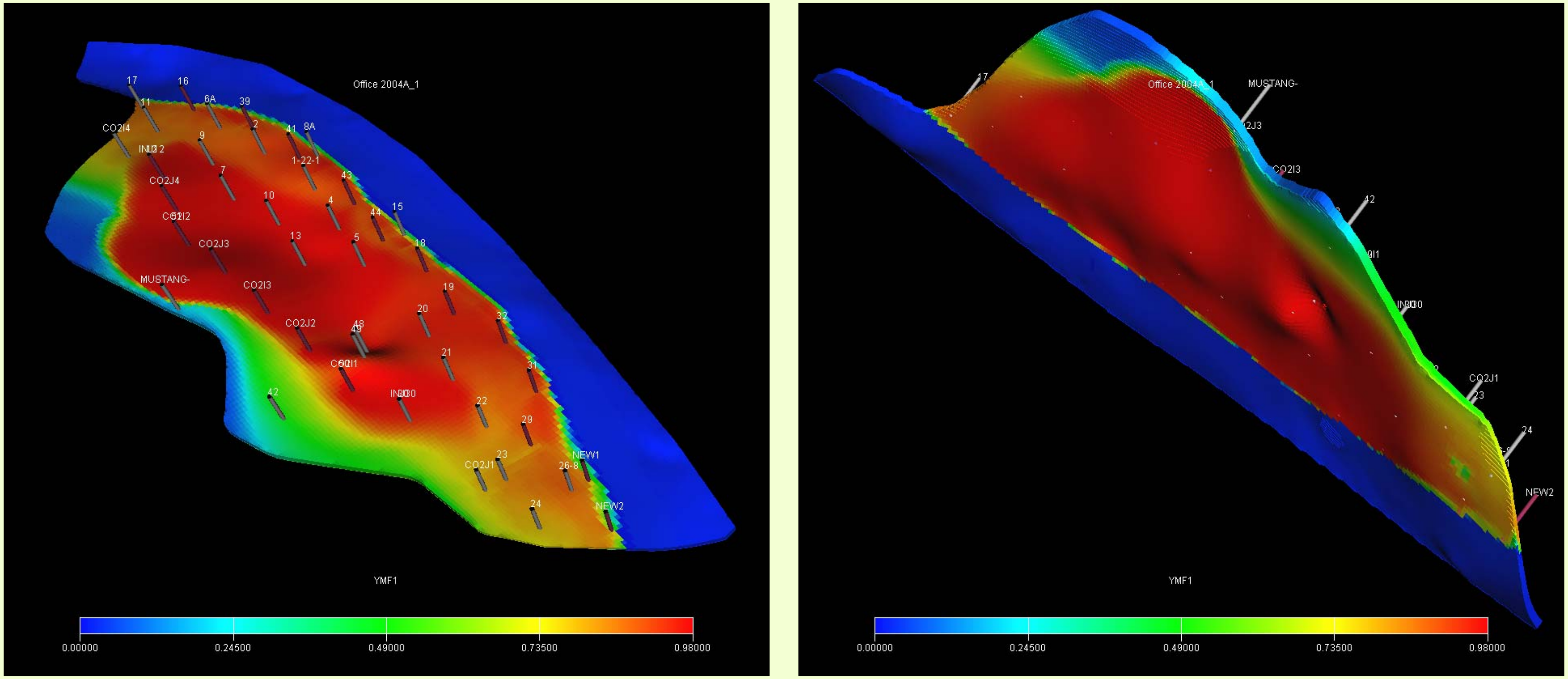

Figure 49. CO2 fraction in the gas phase at the end of a 30-year CO2 flooding in Scenario 3, top view (left) and bottom view (right).

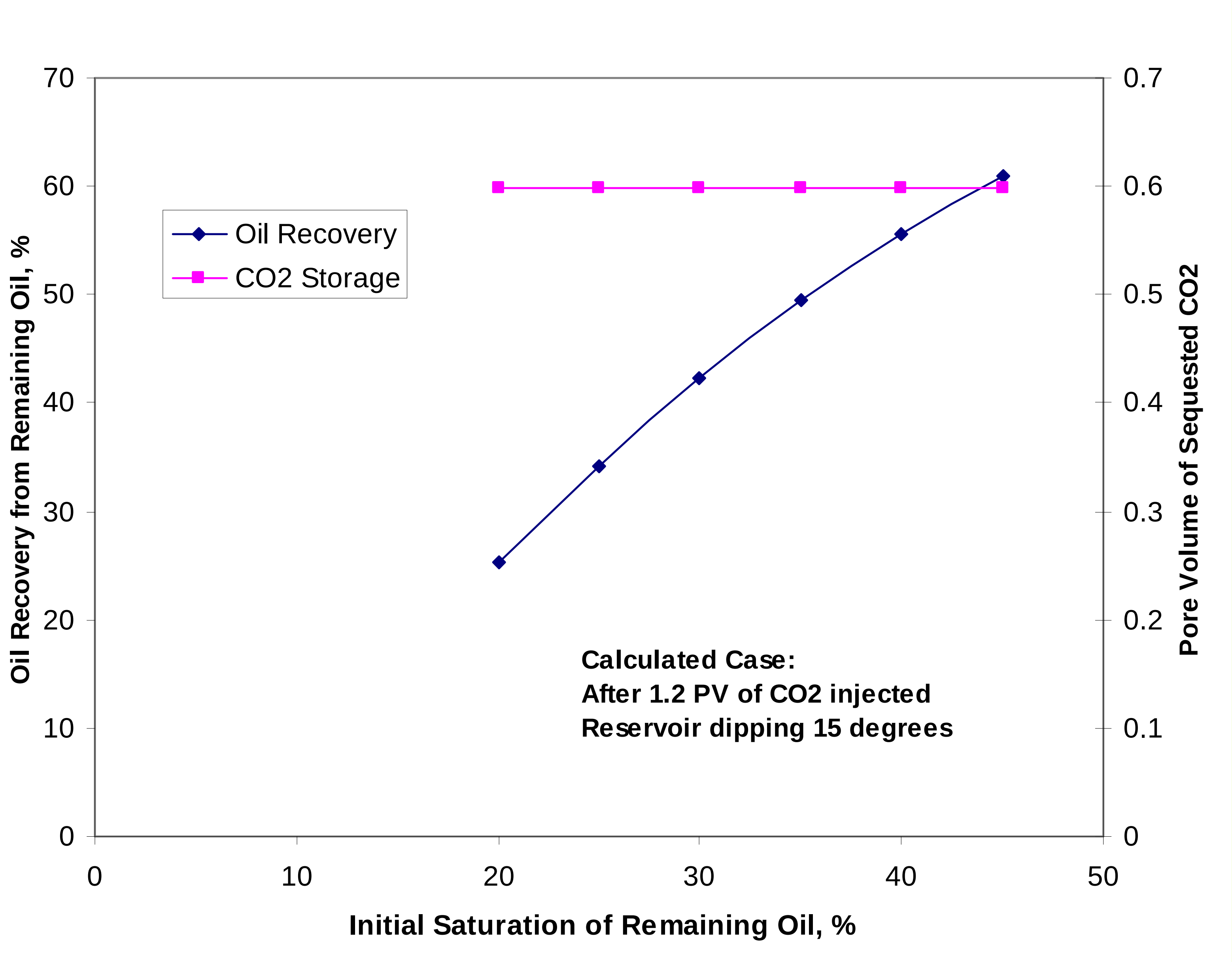

Figure 50. The effect of initial remaining oil saturation on oil recovery by gravity stable CO_2 flood. The calculation was based on the model of Wood *et al* (SPE100021, 2006) with the parameters from the Grieve field configuration.